


RESEARCH ARTICLE

[View Article Online](#)
[View Journal](#) | [View Issue](#)

Cite this: *Med. Chem. Commun.*,
2019, 10, 2146

High affinity rigidified AT₂ receptor ligands with indane scaffolds†

Charlotta Wallinder,^a Christian Sköld,^a Sara Sundholm,^a Marie-Odile Guimond,^c
Samir Yahiaoui,^a Gunnar Lindeberg,^a Nicole Gallo-Payet,^c
Mathias Hallberg ^{*b} and Mathias Alterman^a

Rigidification of the isobutyl side chain of drug-like AT₂ receptor agonists and antagonists that are structurally related to the first reported selective AT₂ receptor agonist 1 (C21) delivered bioactive indane derivatives. Four enantiomer pairs were synthesized and the enantiomers were isolated in an optical purity >99%. The enantiomers **7a**, **7b**, **8a**, **8b**, **9a**, **9b**, **10a** and **10b** bind to the AT₂ receptor with moderate (K_i = 54–223 nM) to high affinity (K_i = 2.2–7.0 nM). The enantiomer with positive optical rotation (+) exhibited the highest affinity at the receptor. The indane derivatives **7b** and **10a** are among the most potent AT₂ receptor antagonists reported so far. As illustrated by the enantiomer pairs **7a/b** and **10a/b**, an alteration at the stereogenic center has a pronounced impact on the activation process of the AT₂ receptor, and can convert agonists to antagonists and *vice versa*.

Received 19th August 2019,
Accepted 30th October 2019

DOI: 10.1039/c9md00402e

rsc.li/medchemcomm

Introduction

The hypertensive octapeptide angiotensin II (Ang II) activates mainly two receptor subtypes; the AT₁ receptor and the AT₂ receptor. Selective AT₁ receptor antagonists have been used as antihypertensives (the Sartans)^{1,2} for more than 25 years, while neither AT₂ receptor agonists nor antagonists have yet been launched as pharmaceuticals. An AT₂ receptor antagonist, EMA401 (olodanrigan) was in clinical trials and aimed for management of neuropathic pain.^{3–5} Moreover, in recent years also AT₂ receptor agonists have emerged as a potential new class of pharmaceutical agents^{5,6} and activation of AT₂ receptor results in a variety of physiological responses.^{6,7} The expression of the AT₂ receptor is often low in healthy adults and is predominately observed in renal, cardiovascular, and brain tissues. However, during certain pathological conditions, such as myocardial infarction, vascular injury, brain ischemia, renal failure, and cutaneous wounds, the AT₂ receptor expression is up-regulated.^{6,7} Notably, receptor activation stimulates neurite outgrowth in

neuronal cells, one of the first steps in neuronal differentiation.⁸

Peptides and pseudopeptides that act as selective AT₂ receptor agonists have been known for a long time and used for comprehensive studies of physiological effects of AT₂ receptor activation.^{9–17}

In 2004, our group disclosed the first selective non-peptide and drug-like receptor AT₂ receptor agonist C21/M024 (**1**)¹⁸ (Fig. 1). Subsequently a series of structurally related agonists were reported.^{19–23} Compound **1** has been evaluated in several experimental disease models and is entering phase II clinical trials as a potential treatment for idiopathic pulmonary fibrosis. For recent reviews and on the discovery of C21 (**1**) and brief surveys of its pharmacology, see references.^{24–26}

We observed that a migration of the methylene imidazole substituent from the *para* position of the agonist **1** to the *meta* position resulted in a compound C38/M132 (**2**) that acted as an AT₂ receptor antagonist.^{27,28} Analogously, the biphenyl derivative **3** that is a potent AT₂ receptor agonist was transformed to the antagonist **4** through the same structural manipulation (Fig. 1).²⁹

Furthermore, we reported that both compound **5** and **6** with the methylene imidazole group in the *para* position and in the *meta* position, respectively, exhibited agonism although their binding affinities to the AT₂ receptor were 10-fold lower. Thus, the relative positions of the methylene imidazole and the isobutyl substituent seemed of importance in determining the functional activity of this class of selective AT₂ receptor biaryl derivatives (Fig. 1).²⁹ It can be

^a Department of Medicinal Chemistry, BMC, Uppsala University, P.O. Box 574, SE-751 23 Uppsala, Sweden

^b The Beijer Laboratory, Department of Pharmaceutical Biosciences, Division of Biological Research on Drug Dependence, BMC, Uppsala University, P.O. Box 591, SE-751 24 Uppsala, Sweden. E-mail: Mathias.Hallberg@farmbio.uu.se

^c Service of Endocrinology, Faculty of Medicine and Health Sciences, University of Sherbrooke, Sherbrooke, J1H 5N4 Quebec, Canada

† Electronic supplementary information (ESI) available: Chiral GC-MS chromatograms of compound **15** and **16**, HPLC purity of the test compounds and computational details. See DOI: 10.1039/c9md00402e

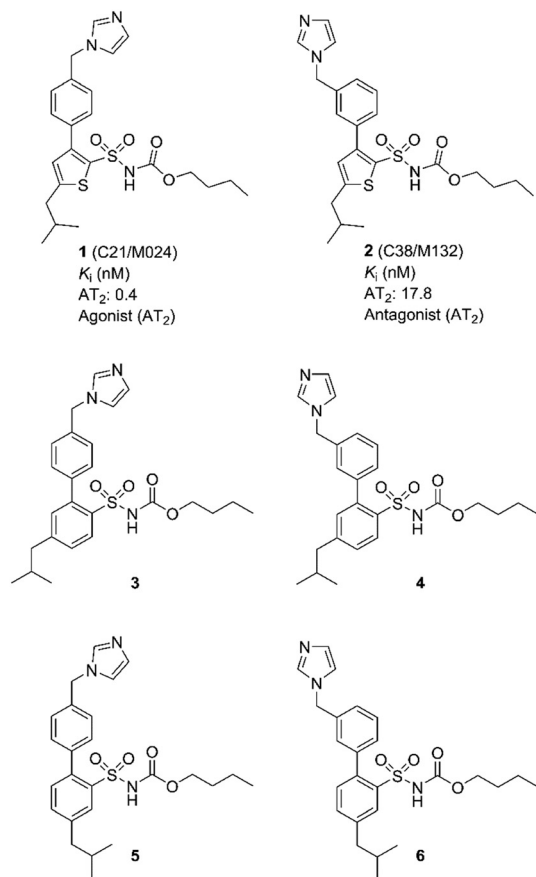


Fig. 1 Structures of compounds 1–6.

hypothesized that the imidazole rings of 1–6 *i.e.* both agonists and antagonists, could bind to the same interaction point of the AT_2 receptor, while the isobutyl groups of agonists and antagonists are forced to be positioned differently and cause the difference in functionality observed. Hence, the topography and location of the lipophilic side chains of 1–6 might be the primary determinants of functionality.

These data and the proposed hypothesis encouraged us to assess the impact and importance of the orientation of the isobutyl side chain in space for a) binding affinity to the AT_2 receptor and b) functional response (agonism or antagonism). It is known that a structurally related non selective AT_1 receptor agonist (L-162782) encompassing the same isobutyl group as in 1–6 was converted to a non selective AT_1 receptor antagonist (L-162389) after deletion of one single methyl group from the side chain.³⁰ Notably, regarding affinity to the AT_1 receptor, there are no examples known of any AT_2 receptor ligand encompassing the imidazole ring that is found in 1–6 that demonstrate any affinity at the AT_1 receptor.

Eight enantiomers, with conformationally constrained isobutyl groups, 7a, 7b, 8a, 8b, 9a, 9b, 10a, 10b, were prepared and their ability to bind to the AT_2 receptor and their capacity to activate or block the AT_2 receptor were

examined (Fig. 2). In essence, there are two classes of ligands: a class with a 1-isopropyl, 4-aryl, 5-sulfonyl arrangement (7 and 8) and a class with a 3-isopropyl, 6-aryl, 5-sulfonyl arrangement (9 and 10) with the aryl group substituted in either the 3'-position or the 4'-position. The isopropyl substituent in each forms a chiral centre.

Results

Chemistry

The synthesis of the rigidified analogues (7a/b, 8a/b, 9a/b and 10a/b) started with the synthesis of 1-isopropylindane (12), which was prepared essentially as described by Phillips *et al.*³¹ Briefly, 1-indanone was alkylated in a Grignard reaction with freshly prepared 2-propylmagnesium bromide. Spontaneous elimination of the alcohol group upon acidic work-up rendered the unsaturated compound 11 which was hydrogenated directly using PtO_2 as the catalyst. The saturated compound 12 was isolated in a total yield of 52%. Compound 12 was subsequently treated with chlorosulfonic acid to yield the positional isomers 13 and 14 in 43%. These two compounds were separated by column chromatography and isolated in 16% and 14% yield, respectively. The isolated sulfonyl chlorides 13 and 14 were directly protected with *tert*-butylamine to provide the sulfonamides 15 and 16, in excellent yields. The enantiomers of 15 and 16 were separated using chiral preparative HPLC (Scheme 1).

Chiral GC-MS was used to determine the enantiomeric purity of the isolated (+) (15a and 16a) and (–) (15b and 16b) forms of 15 and 16, which in both cases proved to be >99%. The pure enantiomers were transformed into the corresponding boronic acids by selective *ortho*-lithiation and subsequent boronation and were used in the next step without further purification.³¹ The crude boronic acids were coupled with compounds 17 and 18, which were prepared by the *N*-alkylation of imidazole by 3- and 4-bromobenzylbromide, respectively. The subsequent Suzuki coupling reactions performed by microwave irradiation (150 °C, 5 min)³² afforded compounds 21a/b, 22a/b in Scheme 2 and compounds 24a/b, 25a/b in Scheme 3. Compounds 21a/b and 22a/b were isolated by HPLC as the TFA salts in moderate yields. We were unfortunately not able to isolate the Suzuki products from boronic acids 20a/b. Compounds

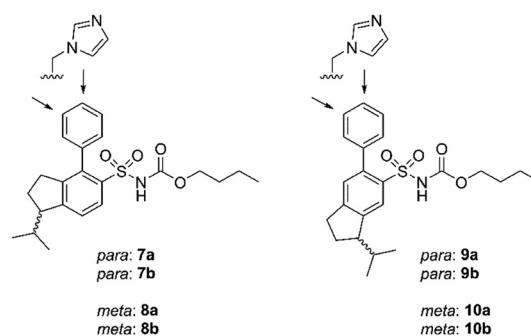
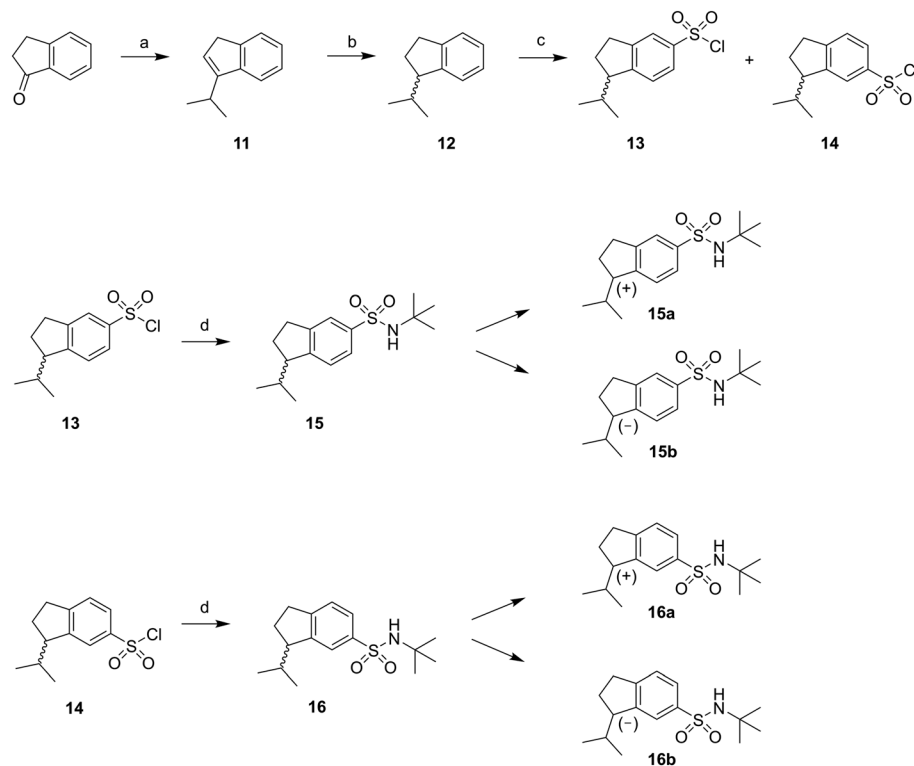
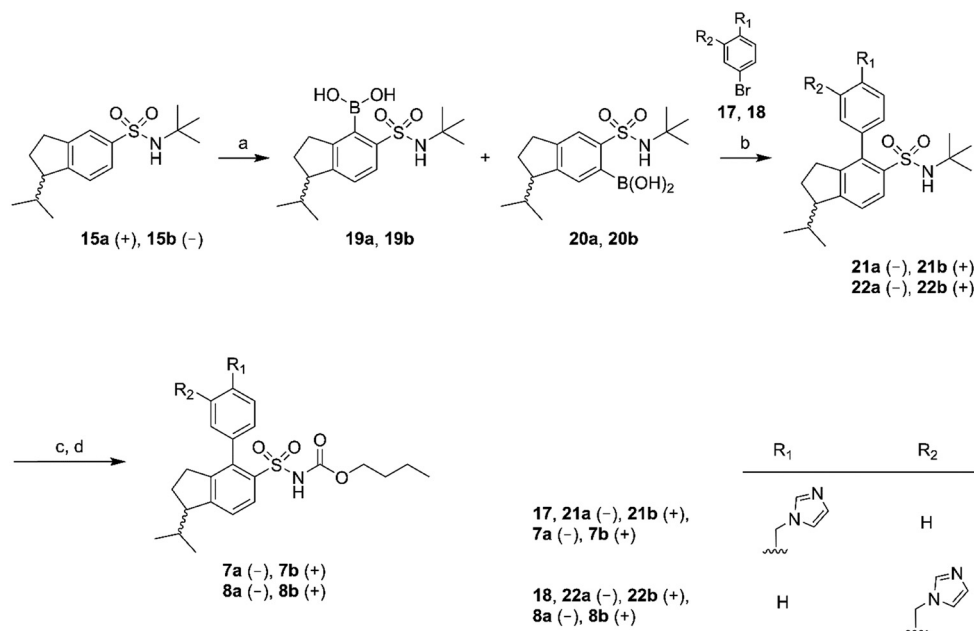


Fig. 2 Structures of compounds 7a/b, 8a/b, 9a/b, 10a/b.





Scheme 1 Reagents: (a) 2-propylmagnesium bromide, diethyl ether, toluene, HCl (aq); (b) H₂ (40 psi), PtO₂, ethanol; (c) chlorosulfonic acid, DCM; (d) *tert*-butylamine, DCM.



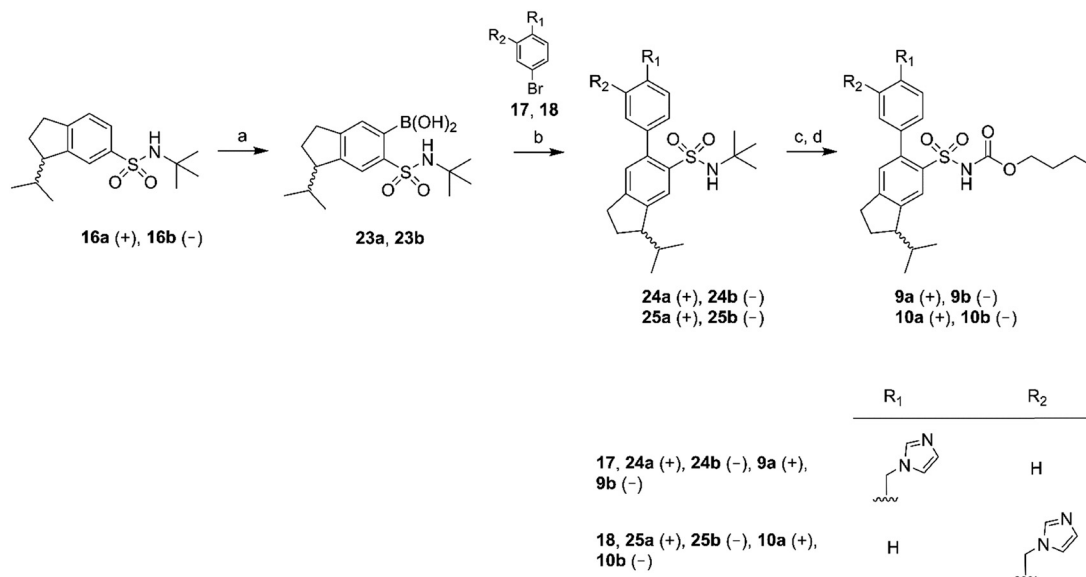
Scheme 2 Reagents: (a) *n*-BuLi, THF, triisopropyl borate, HCl (aq); (b) Pd(PPh₃)₄, Na₂CO₃, toluene, ethanol, H₂O; (c) BCl₃, DCM; (d) *n*-butyl chloroformate, Na₂CO₃, DCM, H₂O.

16a and 16b gave rise to only one boronic acid each (compounds 23a and 23b), probably due to steric hindrance induced by the isopropyl group (Scheme 3).

All isolated Suzuki products (21a/b, 22a/b, 24a/b and 25a/b) were deprotected with BCl₃ (ref. 33) and

subsequently acylated with *n*-butyl chloroformate in dichloromethane, water and Na₂CO₃ to yield the final products 7a/b, 8a/b, 9a/b and 10a/b in 48–61% yield, after purification by preparative HPLC (Schemes 2 and 3).





Scheme 3 Reagents: (a) *n*-BuLi, THF, triisopropyl borate, HCl (aq); (b) Pd(PPh₃)₄, Na₂CO₃, toluene, ethanol, H₂O; (c) BCl₃, DCM; (d) *n*-butyl chloroformate, Na₂CO₃, DCM, H₂O.

Binding assay

The indane analogues, compounds 7a/b, 8a/b, 9a/b and 10a/b, were evaluated for AT₂ receptor affinity in radio-ligand assays by displacement of [¹²⁵I]Ang II from AT₂ receptors in pig uterus membrane as previously described.³⁴ The natural substrate Ang II and the selective AT₁ receptor antagonist losartan were used as reference substances.³⁵ The evaluation of the rigidified enantiomers was focused on AT₂ receptor affinity, since we previously observed that no affinity to the AT₁ receptor is retained when modifying the lower part of this structure class.¹⁹ The results of the binding studies are presented in Table 1. In summary, the 1-isopropyl, 4-aryl, 5-sulfonyl arrangement is less suited to binding than the 3-isopropyl, 6-aryl, 5-sulfonyl arrangement, which all retain potent affinity. C21 (1) exhibited a K_i value of 0.4 nM in the same assay, as previously reported.¹⁸

Functional assay

All rigidified compounds were evaluated for functionality in a neurite outgrowth assay with NG108-15 cells. We have previously shown that NG108-15 cells express mainly the AT₂

receptor and that a three-day treatment with Ang II or the selective peptidic AT₂ receptor agonist CGP-42112 (*N*_α-nicotinoyl-Tyr-(*N*_α-Cbz-Arg)-Lys-His-Pro-Ile)^{36,37} induces neurite outgrowth.^{8,28}

The signaling pathways involve a sustained increase in Rap1/B-Raf/p42/p44^{mapk} activity and activation of the nitric oxide/guanylyl cyclase/cGMP pathway.^{38,39} Cells were treated in the absence or presence of Ang II, 7a/b, 8a/b, 9a/b and 10a/b. Single concentration determinations were applied. After three days of treatment, cells were examined under a phase-contrast microscope and micrographs were taken. To establish an adequate test concentration, the compounds were evaluated at various concentrations ranging from 0.1 nM to 100 nM. It was only at the highest concentration of compounds 7a/b that any evidence of cell death was observed, and that observation was most probably due to a higher concentration of DMSO (verified by a control test, data not shown). All compounds were tested at a concentration of 10 nM, the antagonists (all but 7b) were also tested at 100 nM to verify that the lack of neurite outgrowth was not attributed to too low concentration and the higher concentration did not change the results (data not shown). Co-incubation with the selective AT₂ receptor antagonist PD 123319 reduced the induced neurite outgrowth, verifying that the effect was mediated through the AT₂ receptor. Treatment with PD 123319 alone did not alter the morphology compared to untreated cells (data not shown), as previously reported.²⁸ The antagonistic effect was verified through co-incubation with Ang II resulting in reduced neurite outgrowth. The functionalities are summarised in Table 1 and an overview is presented in Fig. 6. A brief comparison of the functionalities of the compounds examined is available in the Discussion, *vide infra*. The neurite outgrowth results are shown in Fig. 3 and 4.

Table 1 Biological activities at the AT₂ receptor

Compound	Optical rotation	K _i ± SD (nM)	Function (10 nM)
7a	(-)	127.4 ± 4.6	Agonist
7b	(+)	2.8 ± 0.2	Antagonist
8a	(-)	223.1 ± 5.8	Antagonist
8b	(+)	53.5 ± 1.0	Antagonist
9a	(+)	2.2 ± 0.2	Agonist
9b	(-)	5.9 ± 0.1	Agonist
10a	(+)	3.2 ± 0.1	Antagonist
10b	(-)	7.0 ± 0.2	Agonist



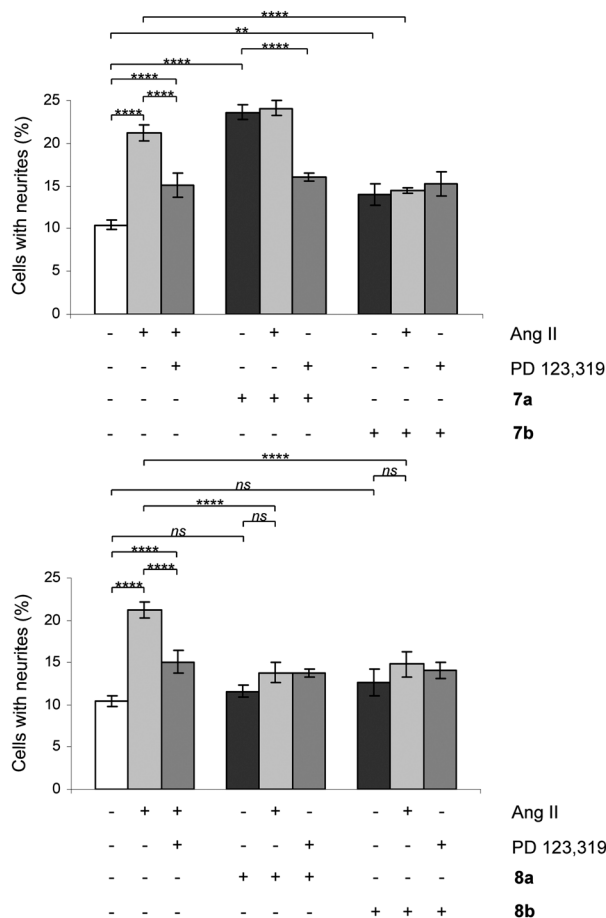


Fig. 3 Effect of compounds **7a/b** and **8a/b** on neurite outgrowth in NG108-15 cells. The cells were plated at a cell density of 3.6×10^4 cells/Petri dishes (35 mm) and were cultured for three days in the absence or presence of 100 nM Ang II, 10 nM **7a**, 10 nM **7b**, 10 nM **8a** or 10 nM **8b** alone or in combination with 10 μ M PD 123319 or 100 nM Ang II. Cells with at least one neurite longer than a cell body were counted as positive for neurite outgrowth. The number of cells with neurites was expressed as the percentage of the total number in the micrographs (at least 400 cells according to the experiment). The results are significant according to two-way ANOVA: ****, $p < 0.0001$; ***, $p < 0.001$; **, $p < 0.01$; ns = not significant.

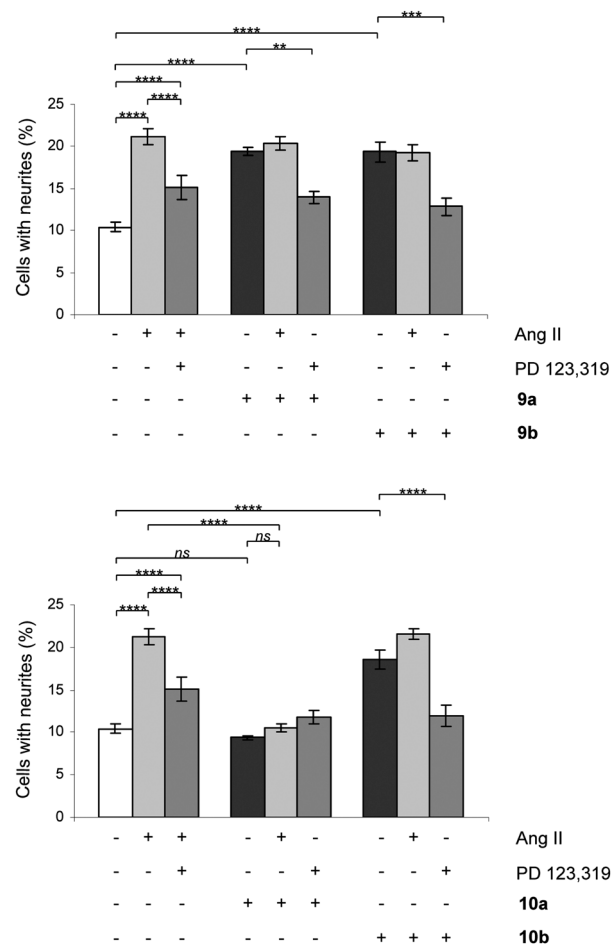


Fig. 4 Effect of compounds **9a/b** and **10a/b** on neurite outgrowth in NG108-15 cells. The cells were plated at a cell density of 3.6×10^4 cells/Petri dishes (35 mm) and were cultured for three days in the absence or presence of 100 nM Ang II, 10 nM **9a**, 10 nM **9b**, 10 nM **10a** or 10 nM **10b** alone or in combination with 10 μ M PD 123319 or 100 nM Ang II. Cells with at least one neurite longer than a cell body were counted as positive for neurite outgrowth. The number of cells with neurites was expressed as the percentage of the total number in the micrographs (at least 400 cells according to the experiment). The results are significant according to two-way ANOVA: ****, $p < 0.0001$; ***, $p < 0.001$; **, $p < 0.01$; ns = not significant.

Discussion

The two rigidified enantiomers **7a** and **7b** displayed large differences in the biological properties as compared to the non rigidified analogue **3**. Compound **7a** (–) lost almost 200 times in affinity, but retained a strong agonistic effect, while the other enantiomer **7b** (+) retained high affinity ($K_i = 2.8$ nM) but the functionality was interconverted to antagonism (Table 1 and Fig. 3). The enantiomer pair **8a/b**, resulting from the rigidification of **4**, both lost affinity compared to **4**, where compound **8a** (–) showed the highest loss. Notably, both compounds retained the antagonistic function (Table 1 and Fig. 3).

Upon rigidification of the biphenyl analogues with the isobutyl chain in the *meta* position in relation to the sulfonylcarbamate group all compounds showed a slightly

higher affinity (Table 1). The enantiomers **9a** and **9b**, resulting from the rigidification of **5**, both retained the agonistic properties. The enantiomer pair from the rigidification of **6**, **10a/b**, on the other hand demonstrated opposite effects, the (–) enantiomer **10b** retained the agonistic effect while the (+) enantiomer **10a** functioned as an antagonist (Table 1 and Fig. 4). Ang II stimulation after pretreatment with **10a** gave the same percentage of neurite outgrowth as untreated control cells, while pretreatment with PD 123319 resulted in a significantly increased number of stimulated cells (****, $p < 0.0001$). This could be an indication that, as previously shown for compound **4**,²⁹ this class of AT₂ receptor antagonists is more efficient in inhibiting Ang II induced neurite outgrowth compared to PD 123319.



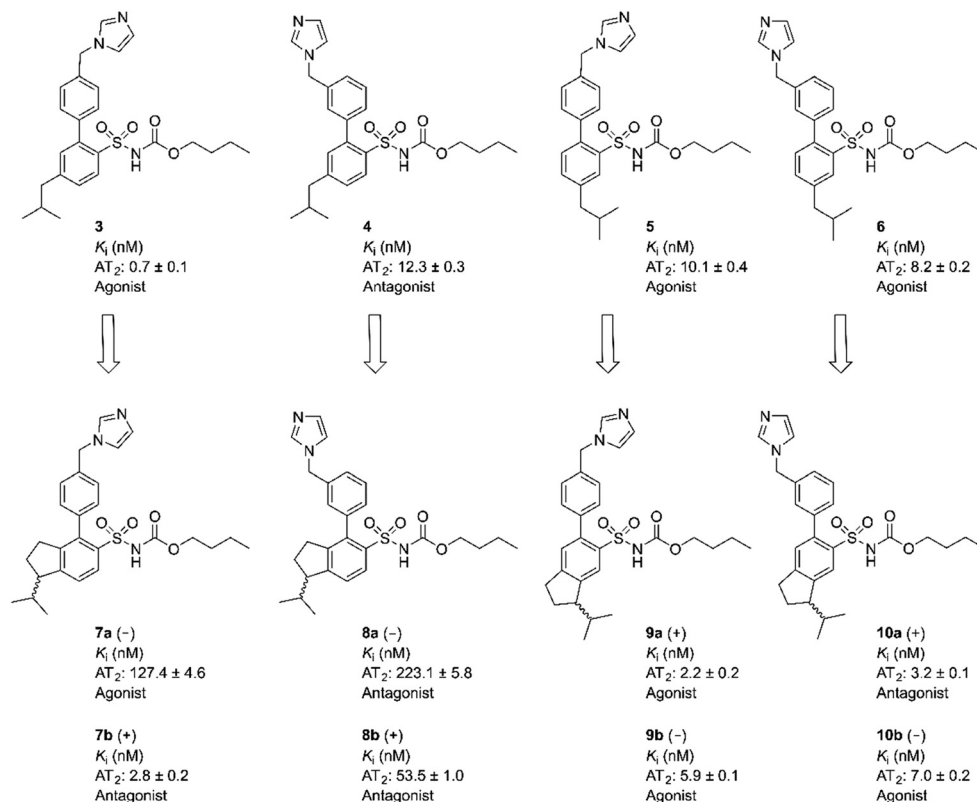


Fig. 5 Overview over the investigated structures and their biological activities at the AT₂ receptor.

From a comparison of the agonist **1** and the antagonist **2** it seems evident that the position of the methyleneimidazole side chain might affect the functional response of this class of compounds.

Thus, the reason for the observed difference in functionality could be attributed to different positions and molecular interactions of the imidazole ring with the AT₂ receptor, when having all other structural features superimposed.

From molecular modeling an alternative hypothesis emerges and suggests that the difference in functionality could instead be due to the positioning of the isobutyl side chain. When the imidazole rings and acidic nitrogen in the sulfonylcarbamate group are superimposed the isobutyl side chains of **1** and **2** are located differently according to modeling. We decided to study this structural feature of AT₂ receptor ligands in some more detail in an attempt to elucidate structural requirements for agonistic and antagonistic response. We reported that independent of the methylene imidazole position, both an antagonist (**4**) and an agonist (**6**) could be obtained by moving the isobutyl side chain.²⁹ This suggests that the structural feature responsible for functionality is the spatial relationship between the imidazole ring and the isobutyl side chain.

To further delineate the structural features important for the functional response, analogues with rigidified alkyl groups mimicking the isobutyl side chain were synthesized and evaluated. The resulting compounds were enantiomeric pairs with different directions of the isobutyl mimicking group, see Table 1 and Fig. 5. In the case of compounds **5** and **6**, with the isobutyl group in the *meta* position to the sulfonylcarbamate group, the rigid analogues **9a/b** and **10a/b** respectively, showed an improved affinity to the receptor, possibly due to an improved fit to the receptor. However, in the case of the *para* substituted isobutyl compounds **3** and **4**, the affinity decreased for the rigidified analogues, **7a/b** and **8a/b** respectively. The agonist **7a** lost nearly 200 times in

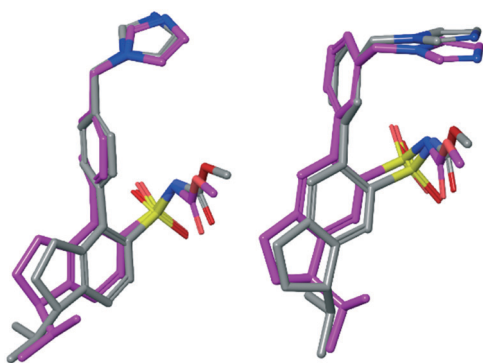


Fig. 6 Low energy conformations of enantiomer pairs superimposed visualizing the small structural difference between an agonist and an antagonist. Left: Model compounds of **7a** (-) (agonist) and **7b** (+) (antagonist) superimposed. Right: Model compounds of **10a** (+) (antagonist) and **10b** (-) (agonist) superimposed.



affinity even though it induced the highest degree of neurite outgrowth among this set of compounds (Fig. 5). A rationale for this observation is not obvious. The antagonist **7b** on the other hand turned out to be the antagonist with the highest affinity found in this compound class. All selective nonpeptide AT₂ receptor antagonists we have reported so far have exhibited lower affinities than the corresponding agonists. The antagonists **7b** and **10a** are indeed the first compounds to show K_i values in the single digit nM range.^{27,29} For comparison the AT₂R antagonists **2** (C38/M132) and **4** display K_i values of 17.8 nM and 12.3 nM, respectively and PD123319 that is structurally very different from the ligands discussed herein exhibits an IC₅₀ of 34 nM.^{18,40}

We have previously observed potent inhibition of Ang II-induced neurite outgrowth from this class of AT₂ receptor antagonists at low concentrations, as compared to the corresponding K_i -values.^{27–29} One hypothesis for this effect may be that a partial inhibition of the signaling pathway is sufficient to completely inhibit neurite outgrowth, the final effect of AT₂ receptor stimulation in NG108-15 cells. This hypothesis is in agreement with the observation that the TrkA inhibitor α -cyano-(3,5-di-*t*-butyl-4-hydroxy)thiocinnamide (AG879)⁴¹ only partially inhibits the p42/p44^{mapk} pathway, but that its effect on neurite outgrowth is total.⁴² When studying the effect of the antagonist **2** on AT₂ receptor signaling pathway a higher level of inhibition was observed at 100 nM compared to 10 nM (inhibition of p42/p44^{mapk} and Rap1), while the difference between the two concentrations was less pronounced in the inhibition of neurite outgrowth induced by Ang II or compound **1** (C21/M024).²⁸ Thus a partial occupation of AT₂ receptor binding sites by these new antagonists could induce partial inhibition of the signaling pathway and, therefore, inhibit Ang II-induced neurite outgrowth. Nevertheless, since the functional experiments were performed on intact cells, the possibility of interactions with other growth stimulating systems cannot be excluded. Thus, not only AT₂R but also interactions with other endogenous receptors might account, at least partly for the observed functional response exerted by this series of compounds.

The present study revealed that the functional response was sensitive to the direction of the isobutyl side chain. In two cases agonists with an isobutyl chain in the *para* and *meta* positions in relation to the sulfonyl carbonate group (**3** and **6**) were rigidified to analogues, which act as antagonists, compound **7b** (+) and compound **10a** (+), respectively. The reason for this is presumably that the bioactive conformation responsible for stabilizing the active conformation of the AT₂ receptor cannot be adopted by **7b** and **10a**.

However, the structural difference between the enantiomers **7a** (agonist) and **7b** (antagonist) and the enantiomers **10a** (antagonist) and **10b** (agonist), respectively, are small. To visualize and exemplify the small structural differences, low energy conformations of model compounds of these enantiomer pairs are shown superimposed in Fig. 6

(see ESI† for details). All-atom superposition resulted in RMSD = 2.64 Å and 3.02 Å for **7a/b** and **10a/b** model structure conformations, respectively. However, the main structural differences clearly reside in the area of the isopropyl substituent, showed by RMSD = 0.62 Å and 0.63 Å, respectively, when excluding the aliphatic part of the indane moiety and the isopropyl substituent in the RMSD calculations. In two cases the functional response was unaffected by rigidification of the isobutyl side chain (**4** to **8a/b** and **5** to **9a/b**, Fig. 6). Thus, the spatial relationship between the structural features in **3** and **6** are sensitive to the direction of the isopropyl group regarding functional response while the spatial arrangement in **4** and **5** render no difference in functionality attributed to the direction of the isopropyl side chain (Fig. 5). This suggests that it is not only the position of the methyleneimidazole, but the spatial relationship between the imidazole ring and the isobutyl side chain that determine the functional activity. Thus, a minor structural alteration can convert these AT₂ receptor ligands from agonists to antagonists. Observations that subtle structural modification is sufficient to convert functionalities of nonpeptide ligands to peptide-activated GPCRs have previously been reported.^{30,43,44}

Concerning peptide-activated GPCRs, and the corresponding endogenous peptide ligands, although the latter are often large, the actual activating or effector domain of the peptide is frequently relatively small and other domains of the full length peptide are required to reach high affinity and selectivity.⁴⁵ The fact that [Ile⁸]AngII acts as an antagonist (or partial agonist) at the AT₁ receptor while the native [Phe⁸]AngII acts an agonist, constitute one example from the renin-angiotensin system (RAS) that small changes in the effector domain of peptides can have a large impact on functionality.⁴⁶ Notable, the classic antihypertensive peptides and AT₁ receptor antagonists saralasin and sarile with lipophilic side chains in the C-terminal, possibly interacting with the same binding site as the isopropyl group of the nonpeptides **7–10** act as agonists at the AT₂ receptor.¹⁵

Conclusion

In summary, it is demonstrated herein that rigidification of the isobutyl side chain, common in AT₂ receptor ligands, by incorporation of an indane scaffold delivers ligands that bind to the AT₂ receptor with moderate to high affinity. In all four cases of enantiomer pairs synthesized and studied (**7a/b**, **8a/b**, **9a/b** and **10a/b**), the enantiomer with positive optical rotation (+) exhibited the highest affinity at the receptor. To the best of our knowledge, **7b** and **10a** are the most potent nonpeptide AT₂ receptor antagonists reported. As illustrated by the enantiomer pairs **7a/b** and **10a/b**, a minor alteration at the stereogenic center can make a great impact on the receptor activation process of the AT₂ receptor, that analogously previously was demonstrated in the case of two AT₁ receptor ligands. Although, we were never able to determine the absolute configuration of the isolated pure



enantiomers, the results presented herein illustrate that small alterations in the topography of the ligands exert a pronounced impact on both affinity and functionality.

Experimental part

Chemistry

General considerations. ^1H (400 MHz) and ^{13}C (100 MHz) NMR spectra were recorded on a Varian Mercury 400 at ambient temperature, if not otherwise stated. Chemical shifts are given as δ values (ppm) downfield from tetramethylsilane and referenced to δ 7.26 and δ 77.16 for CDCl_3 and δ 3.31 and δ 49.00 for CD_3OD . Analytical GC-MS with EI ionization was performed on a Varian 3800 or 3900 equipped with a CP-SIL 5 CB Low Bleed (30 m \times 0.25 mm) or CP-SIL 8 CB Low Bleed (30 m \times 0.25 mm) operating at an ionization energy of 70 eV, using He as carrier gas. The oven temperature was 40–320 $^\circ\text{C}$. Analytical chiral GC-MS was performed on a Varian CP 3800 equipped with a Macherey-Nagel Hydrodex- β -6TBDMS (25 m \times 0.25 mm) column operating at an ionization energy of 70 eV, using He as carrier gas. The oven temperature was 40–320 $^\circ\text{C}$. Analytical RP-HPLC-MS was performed on a Gilson HPLC system equipped with a Zorbax SB C8, 5 μm (4.6 \times 50 mm) column and a Finnigan AQA quadrupole mass spectrometer. The mobile phase consisted of $\text{H}_2\text{O}/\text{MeCN}$ (0.05% HCOOH) and the analyses were run in a gradient mode. Preparative RP-HPLC-MS was performed on a Gilson-Finnigan Thermo Quest AQA system equipped with a Zorbax SB-C8, 5 μm 21.2 \times 150 mm (Agilent technologies) column at a flow rate of 15 mL min^{-1} . The mobile phase consisted of $\text{H}_2\text{O}/\text{MeCN}$ (0.05% HCOOH). Preparative and analytical RP-HPLC was performed on a system consisting of a Gilson 321 pump and a LKB 2151 variable wavelength detector equipped with a Zorbax SB C8 5 μm (21.2 \times 150 mm) column, a ACE 5 Phenyl (150 \times 21.2 mm) and a Zorbax SB C8 5 μm (4.6 \times 50 mm) column, respectively. The mobile phase consisted of $\text{H}_2\text{O}/\text{MeCN}$ with 0.1% TFA or $\text{H}_2\text{O}/\text{MeCN}$ with 0.05% HCOOH . Preparative chiral HPLC-MS was performed on a Gilson-Finnigan Thermo Quest AQA system equipped with a Reprosil-Chiral-NR or a Reprosil-Chiral-NR-R 8 μm (20 \times 250 mm) column. The mobile phase consisted of iso-hexane and 2-propanol. Analytical chiral HPLC was performed on a system consisting of a Gilson 321 pump and a LKB 2151 variable wavelength detector equipped with a Reprosil-Chiral-NR 8 μm (4.6 \times 250 mm) column, using iso-hexane and 2-propanol as mobile phase. Analytical chiral HPLC was also performed on a system consisting of a TSP Spectra Series P200 pump and a Merck/Hitachi L-4000 UV detector equipped with a Reprosil-Chiral-NR or a Reprosil-Chiral-NR-R 8 μm (4.6 \times 250 mm) column, using iso-hexane and 2-propanol as mobile phase. The optical rotation was determined using a Perkin-Elmer 241 polarimeter with chloroform as solvent. Specific rotations ($[\alpha]_D$) are reported in (deg \times mL)/(g \times dm) and the concentration (c) is given in g/100 mL. Microwave heating was performed using Emrys InitiatorTM single mode cavity, producing controlled

irradiation at 2450 MHz. Dedicated microwave vials from Biotage were used for the reactions and the temperature of the reaction mixture was measured using a built-in, on-line infrared temperature sensor. The purity of the test compounds were determined on a Thermo HyPurity C4, 5 μm , 4.6 mm \times 50 mm column and a ACE C18, 5 μm , 4.6 mm \times 50 mm column. Elemental analyses were performed by Analytische Laboratorien, Lindlar, Germany. Exact molecular masses (HRMS) were determined on a Micromass Q-ToF2 mass spectrometer equipped with an electrospray ion source. Dry CH_2Cl_2 was distilled over calcium hydride and dry THF over sodium. Other chemicals and solvents used were of analytical grade and purchased from commercial suppliers, and used without further purification unless stated (e.g. dry THF). Thin-layer chromatography was performed on aluminium plates precoated with silica gel 60 F_{254} (Merck) and visualized with UV light. Flash chromatography was performed on silica gel 60 (0.040–0.063 mm, Merck).

General procedure A, compounds 17 and 18. Bromobenzylbromide and imidazole were dissolved in DMF. The reaction mixture was stirred over night at ambient temperature. The reaction was diluted with 250 mL of water and extracted with CH_2Cl_2 . The combined organic layer was extracted with 1 M HCl and the combined acidic water phase was washed with CH_2Cl_2 . The pH was increased to 8 with saturated Na_2CO_3 and extracted with diethylether. The combined organic layer was washed with brine, dried with K_2CO_3 , filtered and concentrated under vacuum to yield the pure compounds 17 and 18.

1-(4-Bromobenzyl)-1H-imidazole (17). According to the general procedure A, 4-bromobenzylbromide (5.28 g, 0.021 mol) and imidazole (5.80 g, 0.85 mol) were dissolved in 50 mL DMF. Compound 17 was isolated in 72% yield (3.58 g, 0.015 mol) as colourless oil that solidified upon freezing. ^1H NMR (CDCl_3), δ , ppm: 7.70–7.68 (m, 1H), 7.51–7.47 (m, 2H), 7.13–7.12 (m, 1H), 7.05–7.02 (m, 2H), 6.90–6.89 (m, 1H), 5.10 (s, 2H). ^{13}C NMR (CDCl_3), δ , ppm: 137.4, 135.1, 132.4, 129.5, 129.1, 122.6, 119.4, 50.5. Anal. calcd. for $\text{C}_{10}\text{H}_9\text{BrN}_2$: C, 50.66; H, 3.83; N, 11.82. Found: C, 50.63; H, 3.71; N, 11.78.

1-(3-Bromobenzyl)-1H-imidazole (18). According to the general procedure A, 3-bromobenzylbromide (4.02 g, 0.016 mol) and imidazole (4.56 g, 0.67 mol) were dissolved in 50 mL DMF. Compound 18 was isolated in 73% yield (2.75 g, 0.012 mol) as colourless oil. ^1H NMR (CDCl_3), δ , ppm: 7.54–7.53 (m, 1H), 7.46–7.43 (m, 1H), 7.29 (dd, J = 1.9, 1.9 Hz, 1H), 7.22 (dd, J = 8.0, 8.0 Hz, 1H), 7.11–7.10 (m, 1H), 7.07–7.04 (m, 1H), 6.89–6.88 (m, 1H), 5.08 (s, 2H). ^{13}C NMR (CDCl_3), δ , ppm: 138.6, 137.6, 131.6, 130.7, 130.3, 130.3, 125.9, 123.2, 119.4, 50.2. Anal. calcd. for $\text{C}_{10}\text{H}_9\text{BrN}_2$: C, 50.66; H, 3.83; N, 11.82. Found: C, 50.76; H, 3.86; N, 11.97.

General procedure B, compounds 21a, 21b, 22a, 22b, 24a, 24b, 25a, and 25b. To a cooled ($-78\text{ }^\circ\text{C}$) solution of the *t*-butylsulfonamides 15a, 15b, 16a and 16b in dry THF, was *n*-BuLi (1.6 M in hexane) added under nitrogen atmosphere and stirred for 1 hour. The temperature was raised to $-30\text{ }^\circ\text{C}$ and kept for 3 hours and subsequently decreased to $-40\text{ }^\circ\text{C}$.



Triisopropyl borate was then added. The reaction was stirred over night at room temperature. The reaction was cooled (0 °C) and treated with an excess of 2 M HCl solution. The mixture was extracted with EtOAc and the combined organic phase was washed with water and brine. The organic layer was dried with MgSO₄, filtered and evaporated. The crude products **19a/20a**, **19b/20b**, **23a** and **23b** were then used in the next step without further purification. A microwave vial (2–5 mL) was charged with the crude boronic acid, compound **17** or **18**, toluene, ethanol, 2 M Na₂CO₃ and Pd(PPh₃)₄. The reaction mixture was flushed with nitrogen, sealed and heated by microwave irradiation to 150 °C for 5 min. The reaction mixture was diluted with EtOAc and water. The water phase was extracted with EtOAc and the combined organic phase was washed with water and brine, dried with K₂CO₃ or MgSO₄, filtered and concentrated under vacuum. The crude product was purified by column chromatography and if needed subsequently further purified, and in the cases of product mixtures, separated by preparative RP-HPLC (H₂O/MeCN with 0.05% HCOOH or H₂O/MeCN with 0.1% TFA) to isolate the pure compounds **21a**, **21b**, **22a**, **22b**, **24a**, **24b**, **25a**, and **25b**.

General procedure C, compounds 7a, 7b, 8a, 8b, 9a, 9b, 10a and 10b. The *t*-butyl sulfonamides **21a**, **21b**, **22a**, **22b**, **24a**, **24b**, **25a** and **25b** were dissolved in dry CH₂Cl₂ and cooled to 0 °C and deprotected with an excess of 1.0 M BCl₃ in hexane fractions under nitrogen. The reaction was left at room temperature for 1 hour. The reaction mixture was then evaporated and co-evaporated several times with CHCl₃. The residue was dissolved in CH₂Cl₂ and water (3 : 1). Na₂CO₃ was added and the reaction mixture was cooled to 0 °C and *n*-butyl chloroformate was added and the reaction was left to reach room temperature over night. The reaction mixture was diluted with CHCl₃ organic and the phases were separated. The organic phase was washed with water and brine, dried over MgSO₄ and evaporated. The residue was purified on preparative RP-HPLC (H₂O/MeCN with 0.05% HCOOH) to give the pure products **7a**, **7b**, **8a**, **8b**, **9a**, **9b**, **10a** and **10b**.

1-Isopropylindan-5-sulfonylchloride (13) and 1-isopropylindan-6-sulfonylchloride (14). Compound **12** (4.20 g, 26.2 mmol) was dissolved in CH₂Cl₂ (20 mL). The mixture was stirred and cooled to 0 °C on an ice bath. Chlorosulfonic acid (8.7 mL, 131 mmol) was added drop-wise. The reaction mixture was heated to reflux and stirred for 1 h. After cooling to room temperature, the reaction mixture was poured into a mixture of ice and water (120 mL). The water phase was extracted three times with CHCl₃. The combined organic phase was washed with water and brine, dried over MgSO₄ and evaporated. The residue was purified by column chromatography (isohexane:EtOAc 10 : 1) to provide compound **13** in 16% yield (1.09 g, mmol) and compound **14** in 14% yield (0.98 g, mmol). The total yield of the product mixture reached 43% (2.94 g, 11.4 mmol, **13**:mix:**14** = 1 : 0.8 : 0.9).

General procedure D, compounds 15 and 16. Compounds **13** and **14** were dissolved in CH₂Cl₂ (10 mL) and the solution

was cooled on an ice bath to 0 °C. *tert*-Butylamine was added drop-wise and the reaction mixture was stirred at 0 °C for 10 min followed by 1 h at room temperature. The mixture was washed with water and brine, and the organic phase was dried over K₂CO₃. The solvent was removed under vacuum to give the pure compounds **15** and **16**. The racemates were dissolved in a 4 : 1 mixture of isohexane and isopropanol and separated on chiral, preparative HPLC (isohexane/isopropanol 95 : 5 for compound **15** and 93 : 7 for compound **16**) to give the pure enantiomers **15a**, **15b**, **16a** and **16b**. The enantiomeric purity of all isolated enantiomers were >99% according to chiral GC-MS (see ESI† for chromatograms).

***N*-tert-Butyl-1-isopropylindan-5-sulfonamide (15a and 15b).** According to general procedure D compound **13** (1.08 g, 4.2 mmol) was dissolved in CH₂Cl₂ and reacted with *tert*-butylamine (1.75 mL, 16.7 mmol) rendering the pure compound **15** as a white solid in 96% yield (1.19 g, 4.02 mmol). Chiral HPLC separation, performed on totally 1.54 g (5.22 mmol), yielded the pure enantiomers **15a** in 27% yield (415 mg, 1.40 mmol) and **15b** in 26% yield (407 mg, 1.38 mmol) (**15a**:mix:**15b**, 1 : 1 : 1). **15a**: [α]_D²² = +11.7° (c, 1.025, CHCl₃); **15b**: [α]_D²² = -12.2° (c, 1.080, CHCl₃). ¹H NMR (CDCl₃), δ , ppm: 7.70–7.67 (m, 2H), 7.27–7.24 (m, 1H), 4.53 (brs, 1H), 3.17–3.12 (m, 1H), 2.98–2.81 (m, 2H), 2.18–2.08 (m, 2H), 1.96–1.87 (m, 1H), 1.23 (s, 9H), 1.00 (d, *J* = 7.0 Hz, 3H), 0.76 (d, *J* = 7.0 Hz, 3H). ¹³C NMR (CDCl₃), δ , ppm: 151.6, 145.8, 141.4, 125.2, 124.6, 123.0, 54.7, 51.2, 31.7, 30.9, 30.3, 26.6, 21.2, 17.7. Anal. calcd. for C₁₆H₂₅NO₂S: C, 65.05; H, 8.53; N, 4.47. Found (**15a**): C, 64.87; H, 8.52; N, 4.61. Found (**15b**): C, 65.14; H, 8.66; N, 4.56.

***N*-tert-Butyl-1-isopropylindan-6-sulfonamide (16a and 16b).** According to general procedure D compound **14** (0.970 g, 3.7 mmol) was dissolved in CH₂Cl₂ and reacted with *tert*-butylamine (1.6 mL, 15.2 mmol) rendering the pure compound **16** as a white solid in 99% yield (1.10 g, 3.7 mmol). Chiral HPLC separation yielded the pure enantiomers **16a** in 30% yield (323 mg, 1.09 mmol) and **16b** in 24% yield (267 mg, 0.9 mmol) (**16a**:mix:**16b**, 1 : 0.5 : 0.8). **16a**: [α]_D²³ = +33.4° (c, 0.800, CHCl₃); **16b**: [α]_D²³ = -32.7° (c, 1.045, CHCl₃). ¹H NMR (CDCl₃), δ , ppm: 7.69–7.65 (m, 2H), 7.29–7.25 (m, 1H), 4.52 (brs, 1H), 3.18–3.13 (m, 1H), 2.98–2.81 (m, 2H), 2.20–2.08 (m, 2H), 1.95–1.86 (m, 1H), 1.21 (s, 9H), 1.00 (d, *J* = 6.8 Hz, 3H), 0.76 (d, *J* = 6.8 Hz, 3H). ¹³C NMR (CDCl₃), δ , ppm: 149.8, 147.6, 141.2, 125.6, 124.8, 123.1, 54.6, 51.0, 31.9, 30.9, 30.3, 26.7, 21.1, 17.7. Anal. calcd. for C₁₆H₂₅NO₂S: C, 65.05; H, 8.53; N, 4.47. Found (**16a**): C, 64.89; H, 8.43; N, 4.43. Found (**16b**): C, 64.83; H, 8.57; N, 4.54.

***N*-tert-Butyl-4-[4-(imidazol-1-yl)-methylphenyl]-1-isopropylindan-5-sulfonamide (21a).** According to general procedure B compound **15a** (405 mg, 1.37 mmol) was dissolved in dry THF (6 mL) and reacted with *n*-BuLi (2.1 mL, 1.6 M, 3.43 mmol). Afterwards triisopropyl borate (0.50 mL, 2.17 mmol) was added. Two microwave vials (2–5 mL) were charged with the crude mixture of boronic acids **19a** and **20a** (totally 240 mg, <0.70 mmol), compound **17** (338 mg, 1.43 mmol), toluene (2 × 3.5 mL), ethanol (2 × 0.5 mL), Na₂CO₃ (2



M, 2×0.70 mL, 2×1.40 mmol) and $\text{Pd}(\text{PPh}_3)_4$ (2×20 mg, 0.018 mmol). The crude product mixture was purified by column chromatography (CHCl_3 :MeOH, 20:1) and about half of the product mixture was subsequently separated by RP-HPLC ($\text{H}_2\text{O}/\text{MeCN}$ with 0.1% TFA) to yield the pure compound 21a as the TFA salt in >13% (53 mg, 0.094 mmol). An analytical sample was desalted by washing with 2 M Na_2CO_3 for determination of optical rotation and NMR analysis. $[\alpha]_{\text{D}}^{21} = -23.6^\circ$ (c, 0.315, CHCl_3). ^1H NMR (CDCl_3), δ , ppm: 7.98 (d, $J = 8.1$ Hz, 1H), 7.59–7.58 (m, 1H), 7.39–7.37 (m, 1H), 7.34–7.32 (m, 1H), 7.26 (dd, $J = 8.1, 1.0$ Hz, 1H), 7.24–7.19 (m, 2H), 7.13–7.12 (m, 1H), 6.95–6.94 (m, 1H), 5.18 (s, 2H), 3.43 (s, 1H), 3.22–3.17 (m, 1H), 2.53–2.40 (m, 2H), 2.22–2.11 (m, 1H), 2.09–2.00 (m, 1H), 1.85–1.76 (m, 1H), 1.07 (s, 9H), 1.01 (d, $J = 6.8$ Hz, 3H), 0.78 (d, $J = 6.8$ Hz, 3H). ^{13}C NMR (CDCl_3), δ , ppm: 151.5, 146.0, 140.1, 138.1, 137.6, 136.1, 135.2, 130.7, 130.6, 130.2, 127.0, 126.95, 126.90, 123.6, 119.5, 54.6, 51.6, 50.6, 31.6, 30.8, 30.1, 26.3, 21.2, 17.7. HRMS ($\text{M} + \text{H}^+$): 452.2366 $\text{C}_{26}\text{H}_{34}\text{N}_3\text{O}_2\text{S}$ requires 452.2372.

***N*-tert-Butyl-4-[4-(imidazol-1-yl)-methylphenyl]-1-isopropylindan-5-sulfonamide (21b).** According to general procedure B compound 15b (397 mg, 1.34 mmol) was dissolved in dry THF (6 mL) and reacted with *n*-BuLi (2.1 mL, 1.6 M, 3.36 mmol). Afterwards triisopropyl borate (0.50 mL, 2.17 mmol) was added. Two microwave vials (2–5 mL) were charged with the crude mixture of boronic acids 19b and 20b (totally 248 mg, <0.72 mmol), compound 17 (343 mg, 1.45 mmol), toluene (2×3.5 mL), ethanol (2×0.5 mL), Na_2CO_3 (2 M, 2×0.72 mL, 2×1.44 mmol) and $\text{Pd}(\text{PPh}_3)_4$ (2×22 mg, 0.019 mmol). The crude product mixture was purified by column chromatography (CHCl_3 :MeOH, 20:1) and about half of the product mixture was subsequently separated by RP-HPLC ($\text{H}_2\text{O}/\text{MeCN}$ with 0.1% TFA) to yield the pure compound 21b as the TFA salt in >14% (58 mg, 0.103 mmol). An analytical sample was desalted by washing with 2 M Na_2CO_3 for determination of optical rotation and NMR analysis. $[\alpha]_{\text{D}}^{22} = +18.2^\circ$ (c, 0.550, CHCl_3). ^1H NMR (CDCl_3), δ , ppm: 7.97 (d, $J = 8.1$ Hz, 1H), 7.59–7.58 (m, 1H), 7.39–7.36 (m, 1H), 7.34–7.31 (m, 1H), 7.26 (dd, $J = 8.1, 0.9$ Hz, 1H), 7.24–7.18 (m, 2H), 7.13–7.11 (m, 1H), 6.96–6.94 (m, 1H), 5.2 (s, 2H), 3.4 (s, 1H), 3.22–3.16 (m, 1H), 2.53–2.40 (m, 2H), 2.22–2.10 (m, 1H), 2.09–1.99 (m, 1H), 1.85–1.75 (m, 1H), 1.07 (s, 9H), 1.01 (d, $J = 6.9$ Hz, 3H), 0.78 (d, $J = 6.9$ Hz, 3H). ^{13}C NMR (CDCl_3), δ , ppm: 151.5, 146.0, 140.1, 138.1, 137.6, 136.1, 135.2, 130.7, 130.5, 130.1, 127.0, 126.9, 126.9, 123.6, 119.5, 54.6, 51.6, 50.6, 31.5, 30.8, 30.1, 26.3, 21.2, 17.7. HRMS ($\text{M} + \text{H}^+$): 452.2377 $\text{C}_{26}\text{H}_{34}\text{N}_3\text{O}_2\text{S}$ requires 452.2372.

***N*-tert-Butyl-4-[3-(imidazol-1-yl)-methylphenyl]-1-isopropylindan-5-sulfonamide (22a).** According to general procedure B compound 15a (405 mg, 1.37 mmol) was dissolved in dry THF (6 mL) and reacted with *n*-BuLi (2.1 mL, 1.6 M, 3.43 mmol). Afterwards triisopropyl borate (0.50 mL, 2.17 mmol) was added. Two microwave vials (2–5 mL) were charged with the crude mixture of boronic acids 19a and 20a (totally 240 mg, <0.70 mmol), compound 18 (331 mg, 1.40 mmol), toluene (2×3.5 mL), ethanol (2×0.5 mL), Na_2CO_3 (2

M, 2×0.70 mL, 2×1.40 mmol) and $\text{Pd}(\text{PPh}_3)_4$ (2×22 mg, 0.019 mmol). The crude product mixture was purified by column chromatography (CHCl_3 :MeOH, 20:1) and about half of the product mixture was subsequently separated by RP-HPLC ($\text{H}_2\text{O}/\text{MeCN}$ with 0.1% TFA) to yield the pure compound 22a as the TFA salt in >19% (74 mg, 0.131 mmol). An analytical sample was desalted by washing with 2 M Na_2CO_3 for determination of optical rotation and NMR analysis. Compound 22a was observed as two rotamers at 24 °C in NMR in the ratio 1:1. Increasing the temperature to 70 °C (CD_3CN) resulted in one set of peaks, a part from one of the methylgroups which had not fully merged. The spectra recorded at 24 °C are reported here. $[\alpha]_{\text{D}}^{22} = -19.8^\circ$ (c, 0.430, CHCl_3). ^1H NMR (CDCl_3 , 24 °C), δ , ppm: 7.99–7.95 (m, 1H), 7.57–7.54 (m, 1H), 7.45–7.39 (m, 1H), 7.34–7.24 (m, 3H), 7.20–7.13 (m, 1H), 7.09–7.07 (m, 1H), 6.97–6.93 (m, 1H), 5.15 (s, 2H), 3.44–3.40 (m, 1H), 3.22–3.16 (m, 1H), 2.54–2.12 (m, 2H), 2.21–2.12 (m, 1H), 2.09–1.98 (m, 1H), 1.85–1.75 (m, 1H), 1.07–1.04 (m, 9H), 1.03–0.99 (m, 3H), 0.80–0.78 (m, 3H). ^{13}C NMR (CDCl_3 , 24 °C), δ , ppm: 151.5, 145.9, 140.03, 140.00, 138.81, 138.74, 137.5, 136.4, 136.3, 135.25, 135.21, 130.1, 129.7, 129.6, 129.5, 129.3, 128.8, 128.7, 127.02, 126, 99, 126.97, 126.94, 123.64, 123.60, 119.4, 54.58, 54.56, 51.63, 51.56, 50.83, 50.81, 31.6, 31.5, 30.9, 30.6, 30.10, 30.08, 26.4, 26.3, 21.22, 21.15, 17.72, 17.68. HRMS ($\text{M} + \text{H}^+$): 452.2371 $\text{C}_{26}\text{H}_{34}\text{N}_3\text{O}_2\text{S}$ requires 452.2372.

***N*-tert-Butyl-4-[3-(imidazol-1-yl)-methylphenyl]-1-isopropylindan-5-sulfonamide (22b).** According to general procedure B compound 15b (397 mg, 1.34 mmol) was dissolved in dry THF (6 mL) and reacted with *n*-BuLi (2.1 mL, 1.6 M, 3.36 mmol). Afterwards triisopropyl borate (0.50 mL, 2.17 mmol) was added. Two microwave vials (2–5 mL) were charged with the crude mixture of boronic acids 19b and 20b (totally 248 mg, <0.72 mmol), compound 18 (342 mg, 1.44 mmol), toluene (2×3.5 mL), ethanol (2×0.5 mL), Na_2CO_3 (2 M, 2×0.72 mL, 2×1.44 mmol) and $\text{Pd}(\text{PPh}_3)_4$ (2×22 mg, 0.019 mmol). The crude product mixture was purified by column chromatography (CHCl_3 :MeOH, 20:1) and about half of the product mixture was subsequently separated by RP-HPLC ($\text{H}_2\text{O}/\text{MeCN}$ with 0.1% TFA) to yield the pure compound 22b as the TFA salt in >22% (91 mg, 0.161 mmol). An analytical sample was desalted by washing with 2 M Na_2CO_3 for determination of optical rotation and NMR analysis. Compound 22b was observed as two rotamers at 24 °C in NMR in the ratio 1:1. Increasing the temperature to 70 °C (CD_3CN) resulted in one set of peaks a part from one of the methylgroups which had not fully merged. The spectra recorded at 24 °C are reported here. $[\alpha]_{\text{D}}^{22} = +18.0^\circ$ (c, 0.615, CHCl_3). ^1H NMR (CDCl_3 , 24 °C), δ , ppm: 7.99–7.97 (m, 1H), 7.68–7.55 (m, 1H), 7.45–7.40 (m, 1H), 7.34–7.25 (m, 3H), 7.21–7.14 (m, 1H), 7.12–7.08 (m, 1H), 6.99–6.94 (m, 1H), 5.16 (s, 2H), 3.40–3.38 (m, 1H), 3.22–3.17 (m, 1H), 2.54–2.33 (m, 2H), 2.22–2.12 (m, 1H), 2.09–1.99 (m, 1H), 1.85–1.76 (m, 1H), 1.06–1.05 (m, 9H), 1.08–1.00 (m, 3H), 0.82–0.77 (m, 3H). ^{13}C NMR (CDCl_3 , 24 °C), δ , ppm: 151.5, 145.9, 140.03, 139.99, 138.8, 138.7, 137.5, 136.34, 136.26, 135.25, 135.20, 130.1,



129.7, 129.6, 129.5, 129.3, 128.82, 128.76, 127.02, 127.00, 126.97, 126.95, 123.64, 123.60, 119.5, 54.58, 54.55, 51.62, 51.55, 50.84, 50.83, 31.56, 31.49, 30.9, 30.6, 30.10, 30.08, 26.4, 26.3, 21.22, 21.15, 17.71, 17.67. HRMS ($M + H^+$): 452.2375 $C_{26}H_{34}N_3O_2S$ requires 452.2372.

***N*-(Butoxycarbonyl)-4-[4-(imidazol-1-yl)-methylphenyl]-1-isopropylindan-5-sulfonamide (7a).** According to general procedure C compound 21a (30.3 mg, 0.054 mmol) was dissolved in CH_2Cl_2 (1.5 mL) and reacted with BCl_3 in hexane (0.29 mL, 0.29 mmol) The residue was dissolved in CH_2Cl_2 (3 mL) and water (1 mL) and reacted with Na_2CO_3 (26 mg, 0.24 mmol) and *n*-butyl chloroformate (9.5 μ L, 0.075 mmol). The crude product was first purified column chromatography ($CHCl_3$:MeOH 10:1) and subsequently by RP-HPLC (H_2O /MeCN with 0.05% HCOOH) to give compound 7a as a white solid in 61% yield (16.1 mg, 0.0325 mmol). The carbon signals from the imidazole were unfortunately not detected in ^{13}C NMR. $[\alpha]_D^{23} = -31.7^\circ$ (c, 0.400, $CHCl_3$). 1H NMR ($CDCl_3$), δ , ppm: 8.12 (d, $J = 8.1$ Hz, 1H), 7.74–7.50 (m, 1H), 7.33 (dd, $J = 8.1, 1.0$ Hz, 1H), 7.29–7.26 (m, 1H), 7.22–7.19 (m, 1H), 7.17–7.13 (m, 2H), 7.04–6.76 (m, 2H), 5.13 (s, 2H), 4.04 (t, $J = 6.6$ Hz, 2H), 3.22–3.17 (m, 1H), 2.49–2.36 (m, 2H), 2.22–2.14 (m, 1H), 2.08–1.99 (m, 1H), 1.85–1.76 (m, 1H), 1.55–1.47 (m, 2H), 1.30–1.22 (m, 2H), 1.02 (d, $J = 6.8$ Hz, 3H), 0.87 (t, $J = 7.3$ Hz, 3H), 0.80 (d, $J = 6.8$ Hz, 3H). ^{13}C NMR ($CDCl_3$), δ , ppm: 153.0, 151.3, 146.3, 138.0, 136.3, 135.4, 135.2, 130.0, 129.6, 129.4, 127.32, 127.26, 123.6, 66.4, 51.8, 51.1, 31.4, 30.77 (CH_2), 30.76 (CH), 26.3, 21.2, 19.0, 17.8, 13.8. HRMS ($M + H^+$): 496.2277 $C_{27}H_{34}N_3O_4S$ requires 496.2270.

***N*-(Butoxycarbonyl)-4-[4-(imidazol-1-yl)-methylphenyl]-1-isopropylindan-5-sulfonamide (7b).** According to general procedure C compound 21b (31 mg, 0.055 mmol) was dissolved in CH_2Cl_2 (1.5 mL) and reacted with BCl_3 in hexane (0.29 mL, 0.29 mmol) The residue was dissolved in CH_2Cl_2 (3 mL) and water (1 mL) and reacted with Na_2CO_3 (26 mg, 0.24 mmol) and *n*-butyl chloroformate (9.8 μ L, 0.077 mmol). The crude product was first purified column chromatography ($CHCl_3$:MeOH 10:1) and subsequently by RP-HPLC (H_2O /MeCN with 0.05% HCOOH) to give compound 7b as a white solid in 61% yield (16.5 mg, 0.0333 mmol). All carbon signals from the imidazole were unfortunately not detected in ^{13}C NMR. $[\alpha]_D^{23} = +30.2^\circ$ (c, 0.365, $CHCl_3$). 1H NMR ($CDCl_3$), δ , ppm: 8.12 (d, $J = 8.1$ Hz, 1H), 7.70–7.46 (m, 1H), 7.35–32 (m, 1H), 7.29–7.26 (m, 1H), 7.22–7.19 (m, 1H), 7.18–7.13 (m, 2H), 7.04–6.76 (m, 2H), 5.11 (s, 1H), 4.04 (t, $J = 6.6$ Hz, 2H), 3.22–3.17 (m, 1H), 2.49–2.36 (m, 2H), 2.22–2.14 (m, 1H), 2.08–1.99 (m, 1H), 1.85–1.76 (m, 1H), 1.54–1.47 (m, 2H), 1.30–1.20 (m, 2H), 1.02 (d, $J = 6.8$ Hz, 3H), 0.88 (t, $J = 7.4$ Hz, 3H), 0.80 (d, $J = 6.8$ Hz, 3H). ^{13}C NMR ($CDCl_3$), δ , ppm: 153.0, 151.4, 146.3, 137.9, 136.3, 135.5, 135.3, 130.0, 129.6, 129.4, 128.6, 127.3, 127.2, 123.6, 119.4, 66.4, 51.8, 51.0, 31.4, 30.70 (CH_2), 30.68 (CH), 26.3, 21.2, 19.0, 17.8, 13.8. HRMS ($M + H^+$): 496.2260 $C_{27}H_{34}N_3O_4S$ requires 496.2270.

***N*-(Butoxycarbonyl)-4-[3-(imidazol-1-yl)-methylphenyl]-1-isopropylindan-5-sulfonamide (8a).** According to general procedure C compound 22a (40 mg, 0.071 mmol) was

dissolved in CH_2Cl_2 (2 mL) and reacted with BCl_3 in hexane (0.35 mL, 0.35 mmol) The residue was dissolved in CH_2Cl_2 (3 mL) and water (1 mL) and reacted with Na_2CO_3 (34 mg, 0.32 mmol) and *n*-butyl chloroformate (13.5 μ L, 0.099 mmol). The crude product was first purified column chromatography ($CHCl_3$:MeOH 10:1) and subsequently by RP-HPLC (H_2O /MeCN with 0.05% HCOOH) to give compound 8a as a white solid in 59% yield (20.8 mg, 0.0420 mmol). Compound 8a was observed as two rotamers at 24 °C in NMR. Due to high temperature sensitivity no high temperature experiments were performed since this was performed on the protected compound (22a) and the spectra recorded at 24 °C are reported here. $[\alpha]_D^{23} = -23.2^\circ$ (c, 0.590, $CHCl_3$). 1H NMR ($CDCl_3$), δ , ppm: 8.20–8.15 (m, 1H), 7.36–7.12 (m, 5H), 7.05–6.84 (m, 2H), 6.78–6.73 (m, 1H), 5.05–4.75 (m, 2H), 4.11–4.00 (m, 2H), 3.25–3.16 (m, 1H), 2.53–2.32 (m, 2H), 2.24–2.14 (m, 1H), 2.09–2.00 (m, 1H), 1.87–1.76 (m, 1H), 1.57–1.50 (m, 2H), 1.32–1.23 (m, 2H), 1.03 (d, $J = 6.8$ Hz, 3H), 0.91–0.86 (m, 3H), 0.83–0.80 (m, 3H). ^{13}C NMR ($CDCl_3$), δ , ppm: 152.5, 152.41, 152.37, 145.93, 145.92, 138.7, 138.6, 137.0, 136.4, 136.3, 136.0, 135.99, 135.54, 135.50, 129.8, 129.7, 129.2, 129.1, 128.9, 128.7, 128.61, 128.58, 127.8, 125.54, 125.51, 123.5, 119.4, 65.94, 65.90, 51.80, 51.76, 51.00, 31.3, 30.84, 30.80, 30.62, 26.34, 26.30, 21.2, 19.0, 17.9, 17.8, 13.8. HRMS ($M + H^+$): 496.2252 $C_{27}H_{34}N_3O_4S$ requires 496.2270.

***N*-(Butoxycarbonyl)-4-[3-(imidazol-1-yl)-methylphenyl]-1-isopropylindan-5-sulfonamide (8b).** According to general procedure C compound 22b (41 mg, 0.073 mmol) was dissolved in CH_2Cl_2 (2 mL) and reacted with BCl_3 in hexane (0.35 mL, 0.35 mmol). The residue was dissolved in CH_2Cl_2 (3 mL) and water (1 mL) and reacted with Na_2CO_3 (35 mg, 0.33 mmol) and *n*-butyl chloroformate (13.9 μ L, 0.10 mmol). The crude product was first purified column chromatography ($CHCl_3$:MeOH 10:1) and subsequently by RP-HPLC (H_2O /MeCN with 0.05% HCOOH) to give compound 8b as a white solid in 48% yield (17.2 mg, 0.0347 mmol). Compound 8b was observed as two rotamers at 24 °C in NMR. Due to high temperature sensitivity no high temperature experiments were performed since this was performed on the protected compound (22b) and the spectra recorded at 24 °C are reported here. $[\alpha]_D^{23} = +22.8^\circ$ (c, 0.555, $CHCl_3$). 1H NMR ($CDCl_3$), δ , ppm: 8.20–8.15 (m, 1H), 7.36–7.12 (m, 5H), 7.05–6.84 (m, 2H), 6.79–6.74 (m, 1H), 5.04–4.76 (m, 2H), 4.12–4.00 (m, 2H), 3.25–3.16 (m, 1H), 2.53–2.32 (m, 2H), 2.24–2.15 (m, 1H), 2.09–2.00 (m, 1H), 1.87–1.76 (m, 1H), 1.57–1.50 (m, 2H), 1.33–1.22 (m, 2H), 1.03 (d, $J = 6.8$ Hz, 3H), 0.91–0.86 (m, 3H), 0.83–0.80 (m, 3H). ^{13}C NMR ($CDCl_3$), δ , ppm: 152.6, 152.30, 152.25, 146.0, 145.9, 138.63, 138.60, 137.0, 136.4, 136.3, 136.0, 135.9, 135.63, 135.60, 129.8, 129.7, 129.2, 129.1, 128.9, 128.7, 128.63, 128.60, 128.1, 125.58, 125.56, 123.5, 119.4, 66.0, 51.81, 51.77, 50.9, 31.37, 31.35, 30.83, 30.80, 30.63, 26.35, 26.30, 21.3, 19.04, 19.03, 17.9, 17.8, 13.8. HRMS ($M + H^+$): 496.2264 $C_{27}H_{34}N_3O_4S$ requires 496.2270.

***N*-tert-Butyl-5-[4-(imidazol-1-yl)-methylphenyl]-1-isopropylindan-6-sulfonamide (24a).** According to general procedure B compound 16a (292 mg, 0.990 mmol) was



dissolved in dry THF (4 mL) and reacted with *n*-BuLi (1.6 mL, 1.6 M, 2.56 mmol). Afterwards triisopropyl borate (0.35 mL, 1.52 mmol) was added. A microwave vial (2–5 mL) was charged with the crude mixture of boronic acid 23a (110 mg, <0.320 mmol), compound 17 (153 mg, 0.645 mmol), toluene (3.5 mL), ethanol (0.5 mL), Na₂CO₃ (2 M, 0.65 mL, 1.30 mmol) and Pd(PPh₃)₄ (19.0 mg, 16.4 μmol). The crude product was purified twice by column chromatography (CHCl₃:MeOH, 20:1) and subsequently by RP-HPLC (H₂O/MeCN with 0.05% HCOOH) to yield the pure compound 24a as a white solid in >22% (31.2 mg, 0.069 mmol). [α]_D²³ = +13.5° (c, 0.455, CHCl₃). ¹H NMR (CDCl₃), δ , ppm: 7.94 (d, *J* = 1.1 Hz, 1H), 7.72–7.69 (m, 1H), 7.51–7.48 (m, 2H), 7.21–7.24 (m, 2H), 7.12–7.13 (m, 1H), 7.06–7.07 (m, 1H), 6.94–6.95 (m, 1H), 5.19 (s, 2H), 3.53 (s, 1H), 3.23–3.18 (m, 1H), 2.98–2.82 (m, 2H), 2.23–2.12 (m, 2H), 1.98–1.89 (m, 1H), 1.02 (d, *J* = 6.8 Hz, 3H), 0.99 (s, 9H), 0.79 (d, *J* = 6.8 Hz, 3H). ¹³C NMR (CDCl₃), δ , ppm: 149.3, 146.8, 140.5, 140.0, 137.6, 137.4, 135.9, 130.8, 129.4, 128.2, 127.0, 124.3, 119.5, 54.4, 51.0, 50.8, 31.8, 30.8, 29.9, 26.6, 21.1, 17.7. HRMS (M + H⁺): 452.2363, C₂₆H₃₄N₃O₂S requires 452.2372.

***N*-tert-Butyl-5-[4-(imidazol-1-yl)-methylphenyl]-1-isopropylindan-6-sulfonamide (24b).** According to general procedure B compound 16b (256.1 mg, 0.870 mmol) was dissolved in dry THF (3.5 mL) and reacted with *n*-BuLi (1.4 mL, 1.6 M, 2.24 mmol). Afterwards triisopropyl borate (0.30 mL, 1.30 mmol) was added. A microwave vial (2–5 mL) was charged with the crude mixture of boronic acid 23b (95 mg, <0.280 mmol), compound 17 (129 mg, 0.544 mmol), toluene (3.5 mL), ethanol (0.5 mL), Na₂CO₃ (2 M, 0.56 mL, 1.12 mmol) and Pd(PPh₃)₄ (16.2 mg, 14.0 μmol). The crude product was purified twice by column chromatography (CHCl₃:MeOH, 20:1) and subsequently by RP-HPLC (H₂O/MeCN with 0.05% HCOOH) to yield the pure compound 24b as a white solid in >19% (23.4 mg, 0.052 mmol). [α]_D²³ = –13.9° (c, 0.445, CHCl₃). ¹H NMR (CDCl₃), δ , ppm: 7.94 (d, *J* = 1.1 Hz, 1H), 7.69 (m, 1H), 7.51–7.48 (m, 2H), 7.24–7.20 (m, 2H), 7.12–7.13 (m, 1H), 7.07–7.06 (m, 1H), 6.94–6.95 (m, 1H), 5.19 (s, 2H), 3.52 (s, 1H), 3.23–3.18 (m, 1H), 2.98–2.82 (m, 2H), 2.23–2.12 (m, 2H), 1.98–1.89 (m, 1H), 1.02 (d, *J* = 6.8 Hz, 3H), 0.99 (s, 9H), 0.79 (d, *J* = 6.8 Hz, 3H). ¹³C NMR (CDCl₃), δ , ppm: 149.3, 146.8, 140.5, 140.0, 137.6, 137.4, 135.9, 130.8, 129.5, 128.2, 127.0, 124.3, 119.5, 54.4, 51.0, 50.8, 31.8, 30.8, 29.9, 26.6, 21.1, 17.7. HRMS (M + H⁺): 452.2375, C₂₆H₃₄N₃O₂S requires 452.2372.

***N*-tert-Butyl-5-[3-(imidazol-1-yl)-methylphenyl]-1-isopropylindan-6-sulfonamide (25a).** According to general procedure B compound 16a (292 mg, 0.990 mmol) was dissolved in dry THF (4 mL) and reacted with *n*-BuLi (1.6 mL, 1.6 M, 2.56 mmol). Afterwards triisopropyl borate (0.35 mL, 1.52 mmol) was added. A microwave vial (2–5 mL) was charged with the crude mixture of boronic acid 23a (110 mg, <0.320 mmol), compound 18 (158 mg, 0.666 mmol), toluene (3.5 mL), ethanol (0.5 mL), Na₂CO₃ (2 M, 0.65 mL, 1.30 mmol) and Pd(PPh₃)₄ (18.9 mg, 16.4 μmol). The crude product was purified twice by column chromatography

(CHCl₃:MeOH, 20:1) and subsequently by RP-HPLC (H₂O/MeCN with 0.05% HCOOH) to yield the pure compound 25a as a white solid in >21% (29.9 mg, 0.066 mmol). [α]_D²³ = +13.1° (c, 0.470, CHCl₃). ¹H NMR (CDCl₃), δ , ppm: 7.94 (d, *J* = 1.1 Hz, 1H), 7.72–7.67 (m, 1H), 7.45–7.39 (m, 3H), 7.21–7.18 (m, 1H), 7.12–7.08 (m, 1H), 7.07–7.06 (m, 1H), 7.02–6.97 (m, 1H), 5.17 (s, 2H), 3.48 (s, 1H), 3.23–3.18 (m, 1H), 2.98–2.82 (m, 2H), 2.23–2.12 (m, 2H), 1.98–1.89 (m, 1H), 1.02 (d, *J* = 6.8 Hz, 3H), 0.97 (s, 9H), 0.79 (d, *J* = 6.8 Hz, 3H). ¹³C NMR (CDCl₃), δ , ppm: 149.3, 146.8, 141.0, 140.0, 137.6, 137.3, 135.9, 129.9, 129.7, 129.4, 128.7, 128.2, 127.0, 124.4, 119.6, 54.4, 51.12, 51.11, 31.8, 30.8, 29.9, 26.6, 21.1, 17.7. HRMS (M + H⁺): 452.2379, C₂₆H₃₄N₃O₂S requires 452.2372.

***N*-tert-Butyl-5-[3-(imidazol-1-yl)-methylphenyl]-1-isopropylindan-6-sulfonamide (25b).** According to general procedure B compound 16b (256.1 mg, 0.870 mmol) was dissolved in dry THF (3.5 mL) and reacted with *n*-BuLi (1.4 mL, 1.6 M, 2.24 mmol). Afterwards triisopropyl borate (0.30 mL, 1.30 mmol) was added. A microwave vial (2–5 mL) was charged with the crude mixture of boronic acid 23b (95 mg, 0.280 mmol), compound 18 (140 mg, 0.590 mmol), toluene (3.5 mL), ethanol (0.5 mL), Na₂CO₃ (2 M, 0.56 mL, 1.12 mmol) and Pd(PPh₃)₄ (16.2 mg, 14.0 μmol). The crude product was purified twice by column chromatography (CHCl₃:MeOH, 20:1) and subsequently by RP-HPLC (H₂O/MeCN with 0.05% HCOOH) to yield the pure compound 25b as a white solid in >8.9% (11.3 mg, 0.025 mmol). [α]_D²³ = –14.0° (c, 0.400, CHCl₃). ¹H NMR (CDCl₃), δ , ppm: 7.95 (d, *J* = 1.1 Hz, 1H), 7.80–7.79 (m, 1H), 7.44–7.39 (m, 3H), 7.23–7.20 (m, 1H), 7.12–7.11 (m, 1H), 7.07–7.06 (m, 1H), 7.01–7.00 (m, 1H), 5.19 (s, 2H), 3.47 (s, 1H), 3.24–3.19 (m, 1H), 2.98–2.83 (m, 2H), 2.24–2.12 (m, 2H), 1.98–1.90 (m, 1H), 1.02 (d, *J* = 6.8 Hz, 3H), 0.98 (s, 9H), 0.79 (d, *J* = 6.8 Hz, 3H). ¹³C NMR (CDCl₃), δ , ppm: 149.4, 146.9, 141.1, 140.0, 137.6, 137.2, 135.7, 130.0, 129.8, 129.0, 128.8, 128.2, 127.1, 124.5, 119.6, 54.5, 51.2, 51.0, 31.8, 30.9, 30.0, 26.6, 21.1, 17.7. HRMS (M + H⁺): 452.2368, C₂₆H₃₄N₃O₂S requires 452.2372.

***N*-(Butoxycarbonyl)-5-[4-(imidazol-1-yl)-methylphenyl]-1-isopropylindan-6-sulfonamide (9a).** According to general procedure C compound 24a (33.1 mg, 0.073 mmol) was dissolved in CH₂Cl₂ (2 mL) and reacted with BCl₃ in hexane (0.30 mL, 0.30 mmol). The residue was dissolved in CH₂Cl₂ (3 mL) and water (1 mL) and reacted with Na₂CO₃ (36.3 mg, 0.34 mmol) and *n*-butyl chloroformate (12 μL, 0.095 mmol). The crude product was purified by RP-HPLC (H₂O/MeCN with 0.05% HCOOH) to give compound 9a as a white solid in 57% yield (20.7 mg, 0.042 mmol). The carbon signals from the imidazole were unfortunately not detected in ¹³C NMR. [α]_D²³ = +2.9° (c, 0.545, CHCl₃). ¹H NMR (CDCl₃), δ , ppm: 8.06 (d, *J* = 0.9 Hz, 1H), 7.80–7.58 (m, 1H), 7.18–7.13 (m, 3H), 7.37–7.33 (m, 2H), 7.11–6.87 (m, 2H), 5.17 (s, 2H), 4.06–3.96 (m, 2H), 3.26–3.20 (m, 1H), 3.01–2.84 (m, 2H), 2.26–2.13 (m, 2H), 2.02–1.92 (1H), 1.52–1.44 (m, 2H), 1.28–1.17 (m, 2H), 1.05 (d, *J* = 6.8 Hz, 3H), 0.89–0.83 (m, 6H). ¹³C NMR (CDCl₃), δ , ppm: 151.5, 150.7, 146.7, 140.1, 138.8, 135.6, 135.2, 130.2, 128.3, 127.0, 126.6, 66.3, 51.1, 51.0 (detected through HSQC), 31.9,



30.83, 30.75, 26.7, 21.3, 19.0, 17.9, 13.8. HRMS ($M + H^+$): 496.2275 $C_{27}H_{34}N_3O_4S$ requires 496.2270.

N-(Butoxycarbonyl)-5-[4-(imidazol-1-yl)-methylphenyl]-1-isopropylindan-6-sulfonamide (9b). According to general procedure C compound **24b** (23.1 mg, 0.051 mmol) was dissolved in CH_2Cl_2 (1.5 mL) and reacted with BCl_3 in hexane (0.20 mL, 0.20 mmol) The residue was dissolved in CH_2Cl_2 (3 mL) and water (1 mL) and reacted with Na_2CO_3 (25.8 mg, 0.24 mmol) and *n*-butyl chloroformate (8.4 μ L, 0.066 mmol). The crude product was purified by RP-HPLC ($H_2O/MeCN$ with 0.05% $HCOOH$) to give compound **9b** as a white solid in 59% yield (15 mg, 0.030 mmol). The carbon signals from the imidazole were unfortunately not detected in ^{13}C NMR. $[\alpha]_D^{23} = -3.7^\circ$ (*c*, 0.500, $CHCl_3$). 1H NMR ($CDCl_3 + CD_3OD$), δ , ppm: 8.06–8.02 (m, 1H), 7.80–7.48 (m, 1H), 7.36–7.30 (m, 2H), 7.20–6.68 (m, 5H), 5.13 (s, 2H), 4.03–3.93 (m, 2H), 3.23–3.18 (m, 1H), 2.98–2.81 (m, 2H), 2.23–2.11 (m, 2H), 1.98–1.90 (m, 1H), 1.49–1.42 (m, 2H), 1.24–1.15 (m, 2H), 1.03 (d, $J = 6.8$ Hz, 3H), 0.86–0.81 (m, 6H). ^{13}C NMR ($CDCl_3 + CD_3OD$), δ , ppm: 151.1, 150.8, 146.8, 139.8, 138.8, 135.5, 135.3, 130.1, 128.3, 126.8, 126.5, 66.4, 51.1, 51.0 (detected through HSQC), 31.9, 30.8, 30.6, 26.7, 21.2, 18.9, 17.8, 13.7. HRMS ($M + H^+$): 496.2271 $C_{27}H_{34}N_3O_4S$ requires 496.2270.

N-(Butoxycarbonyl)-5-[3-(imidazol-1-yl)-methylphenyl]-1-isopropylindan-6-sulfonamide (10a). According to general procedure C compound **25a** (30.5 mg, 0.068 mmol) was dissolved in CH_2Cl_2 (2 mL) and reacted with BCl_3 in hexane (0.30 mL, 0.30 mmol) The residue was dissolved in CH_2Cl_2 (3 mL) and water (1 mL) and reacted with Na_2CO_3 (34.7 mg, 0.33 mmol) and *n*-butyl chloroformate (11 μ L, 0.088 mmol). The crude product was purified by RP-HPLC ($H_2O/MeCN$ with 0.05% $HCOOH$) to give compound **10a** as a white solid in 61% yield (20.6 mg, 0.042 mmol). The carbon signals from the methyleneimidazole were unfortunately not detected in ^{13}C NMR. $[\alpha]_D^{23} = +8.7^\circ$ (*c*, 0.450, $CHCl_3$). 1H NMR ($CDCl_3$), δ , ppm: 8.13 (s, 1H), 7.50–7.10 (m, 4H), 7.09–6.40 (m, 4H), 4.94 (bs, 2H), 4.12–3.94 (m, 2H), 3.28–3.18 (m, 1H), 3.01–2.82 (m, 2H), 2.29–2.13 (m, 2H), 2.02–1.92 (m, 1H), 1.57–1.46 (m, 2H), 1.32–1.20 (m, 2H), 1.06 (d, $J = 6.8$ Hz, 3H), 0.91–0.78 (m, 6H). ^{13}C NMR ($CDCl_3$), δ , ppm: 151.8, 150.4, 146.6, 140.6, 138.9, 135.9, 135.2, 129.4 (2 CH), 128.3, 128.0, 126.9, 125.7, 66.1, 51.1, 31.9, 30.9 (CH + CH_2), 26.7, 21.3, 19.0, 17.9, 13.8. HRMS ($M + H^+$): 496.2267 $C_{27}H_{34}N_3O_4S$ requires 496.2270.

N-(Butoxycarbonyl)-5-[3-(imidazol-1-yl)-methylphenyl]-1-isopropylindan-6-sulfonamide (10b). According to general procedure C compound **25b** (8.7 mg, 0.019 mmol) was dissolved in CH_2Cl_2 (0.5 mL) and reacted with BCl_3 in hexane (0.08 mL, 0.08 mmol) The residue was dissolved in CH_2Cl_2 (1.5 mL) and water (0.5 mL) and reacted with Na_2CO_3 (11.4 mg, 0.11 mmol) and *n*-butyl chloroformate (3.1 μ L, 0.025 mmol). The crude product was purified by RP-HPLC ($H_2O/MeCN$ with 0.05% $HCOOH$) to give compound **10b** as a white solid in 45% yield (4.2 mg, 8.5 μ mol). $[\alpha]_D^{23} = -8.6^\circ$ (*c*, 0.555, $CHCl_3$). 1H NMR ($CDCl_3$), δ , ppm: 8.13 (d, $J = 0.9$ Hz, 1H), 7.03–24 (m, 4H), 7.06 (m, 1H), 6.95–6.92 (m, 2H), 6.83–6.79 (m, 1H), 4.91 (s, 2H), 4.09–3.98 (m, 2H), 3.23–3.22 (m, 1H),

3.00–2.83 (m, 2H), 2.78–2.14 (m, 2H), 2.01–1.92 (m, 1H), 1.55–1.48 (m, 2H), 1.31–1.21 (m, 2H), 1.06 (d, $J = 6.8$ Hz, 3H), 0.89–0.84 (m, 6H). ^{13}C NMR ($CDCl_3$), δ , ppm: 152.1, 150.4, 146.6, 140.7, 138.9, 137.0, 135.9, 135.0, 129.4 (2 CH), 128.3, 128.0, 127.8, 127.0, 125.7, 119.4, 66.0, 51.12, 50.96, 31.9, 30.8 (CH + CH_2), 26.7, 21.3, 19.0, 17.9, 13.8. HRMS ($M + H^+$): 496.2275 $C_{27}H_{34}N_3O_4S$ requires 496.2270.

Biology

Porcine (pig) myometrial membrane AT_2 receptor-binding assay. Myometrial membranes were prepared from porcine uteri according to the method by Nielsen *et al.*³⁴ A presumable interference by binding to AT_1 receptors was blocked by addition of 1 μ M losartan. Binding of [^{125}I]Ang II to membranes was conducted in a final volume of 0.5 mL containing 50 mM Tris-HCl (pH 7.4), 100 mM NaCl, 10 mM $MgCl_2$, 1 mM EDTA, 0.025% bacitracin, 0.2% BSA, homogenate corresponding to 10 mg of the original tissue weight, [^{125}I]Ang II (80 000–85 000 cpm, 0.03 nM) and variable concentrations of test substance (compounds **7a**, **7b**, **8a**, **8b**, **9a**, **9b**, **10a** and **10b**). Samples were incubated at 25 °C for 1.5 h, and binding was terminated by filtration through Whatman GF/B glass-fiber filter sheets, which had been presoaked overnight with 0.3% polyethylamine, using a Brandel cell harvester. The filters were washed with 3×3 mL of Tris-HCl (pH 7.4) and transferred to tubes. The radioactivity was measured in a γ -counter. The characteristics of the Ang II binding AT_2 receptor was determined by using six different concentrations (0.03–5 nmol L^{-1}) of the labeled [^{125}I]AngII. Nonspecific binding was determined in the presence of 1 μ M Ang II. The specific binding was determined by subtracting the nonspecific binding from the total bound [^{125}I]AngII. The apparent dissociation constant K_i values were calculated from IC_{50} values using the Cheng-Prusoff equation ($K_d = 0.73 \pm 0.06$ nM, $[L] = 0.057$ nM). The binding data were best fitted with a one-site fit. All determinations were performed in triplicate.

General considerations for *in vitro* morphological effects. The chemicals used in the present study were obtained from the following sources: Dulbecco's modified Eagle's medium (DMEM), fetal bovine serum (FBS), HAT supplement (hypoxanthine, aminopterin, thymidine), gentamycin from Gibco BRL (Burlington, Ont, Canada); [Val^5]angiotensin II from Bachem (Marina Delphen, CA, USA). PD123319 was obtained from RBI (Natick, MA, USA). All other chemicals were of grade A purity.

Cell culture. NG108-15 cells (provided by Drs M. Emerit and M. Hamon; INSERM, U. 238, Paris, France) were used to study the *in vitro* morphological effects. In their undifferentiated state, neuroblastoma x glioma hybrid NG108-15 cells have a rounded shape and divide actively. The cells were cultured from passage 18 to 25 in Dulbecco's modified Eagle's medium (DMEM, Gibco BRL, Burlington, Ont., Canada) with 10% fetal bovine serum (FBS, Gibco), HAT supplement and 50 mg L^{-1} gentamycin at 37 °C in 75



cm² Nunclon Delta flasks in a humidified atmosphere of 93% air and 7% CO₂, as previously described.^{8,36} Subcultures were performed at subconfluency. Under these conditions, cells express mainly the AT₂ receptor subtype.^{8,36}

Cells were treated during three days, once a day (first treatment 24 hours after plating), and micrographs were taken the fourth day. For all experiments, cells were plated at the same initial density of 3.6×10^4 cells/35 mm Petri dish. To determine a good test concentration, all compounds were tested at various concentrations ranging from 0.1 nM to 100 nM. It was only at the highest concentration of compounds **7a** and **7b** that any evidence of cell death was observed, and that was most probably due to a higher concentration of DMSO (due to low solubility). Cells were treated without (control cells), or with [Val⁵]-angiotensin II (100 nM) or with compound **7a** (10 nM), **7b** (10 nM), **8a** (10 and 100 nM), **8b** (10 and 100 nM), **9a** (10 nM), **9b** (10 nM), **10a** (10 and 100 nM) or **10b** (10 nM) in the absence or in the presence of PD 123319 (10 μM), an AT₂ receptor antagonist. The antagonist was introduced daily 30 min prior to Ang II, compound **7a**, **7b**, **8a**, **8b**, **9a**, **9b**, **10a** or **10b**. Compound **7a** (10 nM), **7b** (10 nM), **8a** (10 and 100 nM), **8b** (10 and 100 nM), **9a** (10 nM), **9b** (10 nM), **10a** (10 and 100 nM) or **10b** (10 nM) were also tested in the presence of Ang II (100 nM) where the compounds were introduced daily 30 min prior to Ang II, to evaluate antagonistic properties.

Determination of cells with neurites. Cells were examined under a phase contrast microscope and pictures were taken at the end of the experimental period (on the fourth day). Cells with at least one neurite longer than a cell body were counted as positive for neurite outgrowth. The number of cells with neurites was reported as the percentage of the total amount of cells in the micrographs and at least 400 cells were counted in three independent experiments and each condition was performed in duplicate.⁸ The data are represented as mean ± SEM of the average number of cells on a micrograph.

Data analysis. The data are presented as mean ± SEM of the average number of cells on a micrograph. Statistical analyses of the data were performed using the two-way ANOVA test. Homogeneity of variance was assessed by Bartlett's test, and *p* values were obtained from Dunnett's tables.

Conflicts of interest

There are no conflicts to declare.

Acknowledgements

We gratefully acknowledge support from the Swedish Research Council, from the Swedish Foundation for Strategic Research, from Kjell and Märta Beijer Foundation, Knut and Alice Wallenberg Foundation, from the Canadian Institutes of Health Research to N. G. P. and M. D. Payet (MOP 27912), from the Alzheimer's Society of Canada to N. G. P. and by the

program of Canada Research Chair to N. G. P., and Vicore Pharma AB. N. G. P. is a holder of a Canadian Research Chair in Endocrinology of the Adrenal Gland. We also thank Dr. Milad Botros for technical assistance and Dr. Luke R. Odell for linguistic advice.

References

- 1 W. H. Birkenhäger and P. W. de Leeuw, *J. Hypertens.*, 1999, **17**, 873–881.
- 2 M. Burnier, *Circulation*, 2001, **103**, 904–912.
- 3 A. S. C. Rice, R. H. Dworkin, T. D. McCarthy, P. Anand, C. Bountra, P. I. McCloud, J. Hill, G. Cutter, G. Kitson, N. Desem and M. Raff, *Lancet*, 2014, **383**, 1637–1647.
- 4 M. T. Smith, B. D. Wyse and S. R. Edwards, *Pain Med.*, 2013, **14**, 692–705.
- 5 J. M. Keppel Hesselink and M. E. Schatman, *J. Pain Res.*, 2017, **10**, 439–443.
- 6 U. M. Steckelings, E. Kaschina and T. Unger, *Peptides*, 2005, **26**, 1401–1409.
- 7 S. H. Padia and R. M. Carey, *Pflugers Arch.*, 2013, **465**, 99–110.
- 8 L. Laflamme, M. Gasparo, J. M. Gallo, M. D. Payet and N. Gallo-Payet, *J. Biol. Chem.*, 1996, **271**, 22729–22735.
- 9 S. Whitebread, M. Mele, B. Kamber and M. de Gasparo, *Biochem. Biophys. Res. Commun.*, 1989, **163**, 284–291.
- 10 J. Georgsson, U. Rosenstrom, C. Wallinder, H. Beaudry, B. Plouffe, G. Lindeberg, M. Botros, F. Nyberg, A. Karlen, N. Gallo-Payet and A. Hallberg, *Bioorg. Med. Chem.*, 2006, **14**, 5963–5972.
- 11 R. C. Speth and K. H. Kim, *Biochem. Biophys. Res. Commun.*, 1990, **169**, 997–1006.
- 12 U. Rosenström, C. Sköld, B. Plouffe, G. Lindeberg, M. Botros, F. Nyberg, G. Wolf, A. Karlén, N. Gallo-Payet and A. Hallberg, *J. Med. Chem.*, 2005, **48**, 4009–4024.
- 13 F. Magnani, C. G. Pappas, T. Crook, V. Magafa, P. Cordopatis, S. Ishiguro, N. Ohta, J. Selent, S. Bosnyak, E. S. Jones, I. P. Gerothanassis, M. Tamura, R. E. Widdop and A. G. Tzakos, *ACS Chem. Biol.*, 2014, **9**, 1420–1425.
- 14 E. S. Jones, M. P. Del Borgo, J. F. Kirsch, D. Clayton, S. Bosnyak, I. Welungoda, N. Hausler, S. Unabia, P. Perlmutter, W. G. Thomas, M. I. Aguilar and R. E. Widdop, *Hypertension*, 2011, **57**, 570–576.
- 15 M. O. Guimond, M. Hallberg, N. Gallo-Payet and C. Wallinder, *ACS Med. Chem. Lett.*, 2014, **5**, 1129–1132.
- 16 M. Hallberg, J. Savmarker and A. Hallberg, *Curr. Protein Pept. Sci.*, 2017, **18**, 809–818.
- 17 G. T. Wagenaar, H. Laghmani el, M. Fiddler, R. M. Sengers, Y. P. de Visser, L. de Vries, R. Rink, A. J. Roks, G. Folkerts and F. J. Walther, *Am. J. Physiol.*, 2013, **305**, L341–L351.
- 18 Y. Wan, C. Wallinder, B. Plouffe, H. Beaudry, A. K. Mahalingam, X. Wu, B. Johansson, M. Holm, M. Botoros, A. Karlen, A. Pettersson, F. Nyberg, L. Fandriks, N. Gallo-Payet, A. Hallberg and M. Alterman, *J. Med. Chem.*, 2004, **47**, 5995–6008.



- 19 X. Wu, Y. Wan, A. K. Mahalingam, A. M. S. Murugaiah, B. Plouffe, M. Botros, A. Karlén, M. Hallberg, N. Gallo-Payet and M. Alterman, *J. Med. Chem.*, 2006, **49**, 7160–7168.
- 20 A. M. S. Murugaiah, C. Wallinder, A. K. Mahalingam, X. Wu, Y. Wan, B. Plouffe, M. Botros, A. Karlén, M. Hallberg, N. Gallo-Payet and M. Alterman, *Bioorg. Med. Chem.*, 2007, **15**, 7166–7183.
- 21 C. Wallinder, M. Botros, U. Rosenström, M.-O. Guimond, H. Beaudry, F. Nyberg, N. Gallo-Payet, A. Hallberg and M. Alterman, *Bioorg. Med. Chem.*, 2008, **16**, 6841–6849.
- 22 A. K. Mahalingam, Y. Wan, A. M. S. Murugaiah, C. Wallinder, X. Wu, B. Plouffe, M. Botros, F. Nyberg, A. Hallberg, N. Gallo-Payet and M. Alterman, *Bioorg. Med. Chem.*, 2010, **18**, 4570–4590.
- 23 J. Liu, Q. Liu, X. Yang, S. Xu, H. Zhang, R. Bai, H. Yao, J. Jiang, M. Shen, X. Wu and J. Xu, *Bioorg. Med. Chem.*, 2013, **21**, 7742–7751.
- 24 M. Hallberg, C. Sumners, U. M. Steckelings and A. Hallberg, *Med. Res. Rev.*, 2018, **38**, 602–624.
- 25 M. Larhed, M. Hallberg and A. Hallberg, *Med. Chem. Rev.*, 2018, **51**, 69–82.
- 26 Y. Wang, M. Del Borgo, H. W. Lee, D. Baraldi, B. Hirmiz, T. A. Gaspari, K. M. Denton, M. I. Aguilar, C. S. Samuel and R. E. Widdop, *Front. Pharmacol.*, 2017, **8**, 564.
- 27 A. M. S. Murugaiah, X. Wu, C. Wallinder, A. K. Mahalingam, Y. Wan, C. Sköld, M. Botros, M.-O. Guimond, A. Joshi, F. Nyberg, N. Gallo-Payet, A. Hallberg and M. Alterman, *J. Med. Chem.*, 2012, **55**, 2265–2278.
- 28 M.-O. Guimond, C. Wallinder, M. Alterman, A. Hallberg and N. Gallo-Payet, *Eur. J. Pharmacol.*, 2013, **699**, 160–171.
- 29 C. Wallinder, C. Sköld, M. Botros, M.-O. Guimond, M. Hallberg, N. Gallo-Payet, A. Karlén and M. Alterman, *ACS Med. Chem. Lett.*, 2015, **6**, 178–182.
- 30 S. Perlman, C. M. Costa-Neto, A. A. Miyakawa, H. T. Schambye, S. A. Hjorth, A. C. Paiva, R. A. Rivero, W. J. Greenlee and T. W. Schwartz, *Mol. Pharmacol.*, 1997, **51**, 301–311.
- 31 D. D. Phillips, J. A. Cimildoro, P. Scheiner and W. A. Johnson, *J. Org. Chem.*, 1958, **23**, 786–788.
- 32 M. Larhed and A. Hallberg, *J. Org. Chem.*, 1996, **61**, 9582–9584.
- 33 Y. Wan, X. Wu, A. K. Mahalingam and M. Alterman, *Tetrahedron Lett.*, 2003, **44**, 4523–4525.
- 34 A. H. Nielsen, K. Schauser, H. Winther, V. Dantzer and K. Poulsen, *Clin. Exp. Pharmacol. Physiol.*, 1997, **24**, 309–314.
- 35 D. J. Carini, J. V. Duncia, P. E. Aldrich, A. T. Chiu, A. L. Johnson, M. E. Pierce, W. A. Price, J. B. I. Santella, G. J. Wells, R. R. Wexler, P. C. Wong, S.-E. Yoo and P. B. M. W. M. Timmermans, *J. Med. Chem.*, 1991, **34**, 2525–2547.
- 36 B. Buisson, S. P. Bottari, M. de Gasparo, N. Gallo-Payet and M. D. Payet, *FEBS Lett.*, 1992, **309**, 161–164.
- 37 V. Brechler, P. W. Jones, N. R. Levens, M. de Gasparo and S. P. Bottari, *Regul. Pept.*, 1993, **44**, 207–213.
- 38 L. Gendron, L. Laflamme, N. Rivard, C. Asselin, M. D. Payet and N. Gallo-Payet, *Mol. Endocrinol.*, 1999, **13**, 1615–1626.
- 39 L. Gendron, F. Cote, M. D. Payet and N. Gallo-Payet, *Neuroendocrinology*, 2002, **75**, 70–81.
- 40 A. M. Murugaiah, X. Wu, C. Wallinder, A. K. Mahalingam, Y. Wan, C. Skold, M. Botros, M. O. Guimond, A. Joshi, F. Nyberg, N. Gallo-Payet, A. Hallberg and M. Alterman, *J. Med. Chem.*, 2012, **55**, 2265–2278.
- 41 A. Levitzki and A. Gazit, *Science*, 1995, **267**, 1782–1788.
- 42 B. Plouffe, M. O. Guimond, H. Beaudry and N. Gallo-Payet, *Endocrinology*, 2006, **147**, 4646–4654.
- 43 E. E. Sugg, *Annual Reports in Medicinal Chemistry*, 1997, vol. 32, pp. 277–283.
- 44 M. Wijtmans, D. J. Scholten, L. Roumen, M. Canals, H. Custers, M. Glas, M. C. A. Vreeker, F. J. J. de Kanter, C. de Graaf, M. J. Smit, I. J. P. de Esch and R. Leurs, *J. Med. Chem.*, 2012, **55**, 10572–10583.
- 45 J. S. Blakeney, R. C. Reid, G. T. Le and D. P. Fairlie, *Chem. Rev.*, 2007, **107**, 2960–3041.
- 46 M. C. Khosla, R. A. Leese, W. L. Maloy, A. T. Ferreira, R. R. Smeby and F. M. Bumpus, *J. Med. Chem.*, 1972, **15**, 792–795.

